ORNL/TM-5399

Empirical Relationships Among Creep Properties of Four Elevated-Temperature Structural Materials

M. K. Booker
V. K. Sikka

OAK RIDGE NATIONAL LABORATORY
OPERATED BY UNION CARBIDE CORPORATION FOR THE ENERGY RESEARCH AND DEVELOPMENT ADMINISTRATION

DISCLAIMER

Printed in the United States of America. Available from
the Energy Research and Development Administration,
Technical Information Center
P.O. Box 62, Oak Ridge, Tennessee 37830
Price: Printed Copy $5.00 ; Microfiche $2.25

ORNL/TM-5399
UC-79b, -k
(Liquid Metal Fast
Breeder Reactors)

Contract No. W-7405-eng-26

METALS AND CERAMICS DIVISION

EMPIRICAL RELATIONSHIPS AMONG CREEP PROPERTIES OF FOUR ELEVATED-TEMPERATURE STRUCTURAL MATERIALS

M. K. Booker and V. K. Sikka

JUNE 1976

OAK RIDGE NATIONAL LABORATORY
Oak Ridge, Tennessee 37830
operated by
UNION CARBIDE CORPORATION
for the
ENERY RESEARCH AND DEVELOPMENT ADMINISTRATION

THIS PAGE

WAS INTENTIONALLY

LEFT BLANK

CONTENTS

EMPIRICAL RELATIONSHIPS AMONG CREEP PROPERTIES OF FOUR ELEVATED-TEMPERATURE STRUCTURAL MATERIALS

M. K. Booker and V. K. Sikka

ABSTRACT

Elevated-temperature creep and creep-rupture data for four important structural materials are examined to determine empirical relationships among various properties. Materials used include types 304 and 316 austenitic stainless steel, ferritic 2 1/4 Cr-1 Mo steel, and nickel-base Inconel alloy 718. Results obtained allow use of rupture life and minimum creep rate data to predict time to tertiary creep, creep ductility, and creep strain-time response. Such predictions are useful since in general more data are available for rupture life and minimum creep rate than for other properties.

INTRODUCTION

The design of elevated-temperature operating systems requires a careful and thorough consideration of the creep properties of the construction materials involved. Many experimental creep and creep-rupture data are available for a variety of materials, but much of the previous effort in the collection and analysis of such data has been focused only on the time to rupture. However, the actual useful life of a material corresponds not to the rupture life, but to the time period over which the material can exhibit stable or uniform deformation. In recognition of this fact, current elevated-temperature design rules[1] specify three specific criteria that must be considered in the establishment of elevated-temperature time dependent allowable stress levels. According to these rules, the time-dependent allowable stress, S_{mt}, is given by the least of:

1. 2/3 of the minimum stress to cause rupture,
2. 80% of the minimum stress to cause onset of tertiary creep,
3. the minimum stress to cause a total inelastic strain of 1%.

Unfortunately, the data needed to establish the latter two criteria are generally less plentiful than rupture data. Also, methods for analysis of rupture data have been the most studied of the three. One possible solution to these problems might be to establish analytical relationships between rupture life and each of the other criteria. However, since the time to rupture is a failure characteristic, while the time to 1% strain is a flow property, the relationship between these properties may not always be clear. One flow property for which data

are widely available is the minimum creep rate. This report presents the results of exploratory analyses of empirical relationships among rupture life, minimum creep rate, and other creep properties for four important elevated-temperature structural materials. The results and discussion presented here represent both a review of past investigations and an exploration of new relationships. These relationships will be used to illustrate methods for estimating the properties involved in establishing time-dependent design criteria, as well as to estimate creep ductility and creep strain-time behavior.

MATERIALS

Analyses and results are presented here for types 304 and 316 austenitic stainless steel, ferritic 2 1/4 Cr-1 Mo steel, and nickel-base Inconel alloy 718. Tables 1 and 2 describe the material for which the data used were derived. Included are four sets of type 304 stainless steel data,[2—5] two sets of type 316 stainless steel data,[4,6,7] and two sets of Inconel alloy 718 data.[8,9] In some cases, data from various other heats of these materials are used, as indicated. Because of a relative shortage of data for individual heats of 2 1/4 Cr-1 Mo steel, data for several heats[10] were analyzed together. The data for 25.4- and 50.8-mm-thick (1- and 2-in.) plates of type 304 stainless steel heat 9T2796 were analyzed separately because these two forms exhibit significantly different creep behavior. More details about the data will be given as they relate to the specific analyses presented in this report.

TIME TO TERTIARY CREEP

In the following analysis of data for the time to tertiary creep, t_3, two different definitions of the onset of tertiary creep were used. The time to the first deviation from linear second-stage creep is here denoted by t_2, while t_{ss} denotes the time to the onset of tertiary creep as determined by a 0.2% offset from the second-stage creep line. Figure 1 illustrates the determination of t_2 and t_{ss} for a classical creep curve and of t_{ss} for a curve that is concave upward throughout but exhibits a brief linear portion. The quantity t_2 was used for the Garofalo et al.[6,7] data and for heats 55697 and 332990, while t_{ss} was used for the other heats. In the analysis of data for type 304 stainless steel, data from several heats from the ORNL heat-to-heat variations program[11] were utilized, although these heats are not listed in Tables 1 and 2. Both t_{ss} and t_2 were used for those data,[11] since both quantities were available.

Methods for analysis of data for the time to tertiary creep, t_3, were suggested previously.[12] If sufficient data are available, t_3 may be expressed as a function of stress and temperature by the same methods used for the analysis of stress-rupture data.[13—16] However, sometimes available data are inadequate to determine with confidence the relationships among stress, temperature, and t_3. When this situation arises,

Table 1. Compositions and Product Forms of Materials Investigated

Heat	Reference	Product Form	Content, wt %[a]												
			C	Mn	P	S	Si	Cr	Ni	Co	Mo	Cu	N	Nb+Ta	Ti
							Type 304 Stainless Steel								
9T2796	2	25.4-mm plate	0.051	1.37	0.041	b	0.4	18.5	9.87	0.1	0.3	0.24	0.031	b	b
9T2796	3	50.8-mm plate	0.047	1.22	0.029	0.012	0.47	18.5	9.58	0.05	0.10	0.10	0.031	b	b
55697	4	7-mm rod	0.052	1.1	0.011	0.01	0.52	18.92	9.52	0.035	0.12	0.10	0.052	b	b
8043813	5	25.2-mm plate	0.062	1.87	0.04	0.0043	0.48	17.8	8.95	0.20	0.32	0.20	0.033	b	b
ASTM A 240, 479		Plate, rod	0.08[c]	2.0[c]	0.045[c]	0.03[c]	1.0[c]	17–19	8–10						
							Type 316 Stainless Steel								
332390	4	7-mm rod	0.052	1.72	0.012	0.02	0.38	17.8	13.55	0.14	2.33	0.20	0.041	b	b
Garofalo et al.	6,7	12.7-mm bar	0.07	1.94	0.01	0.021	0.38	18.0	11.4	b	2.15	b	0.043	b	b
ASTM A 240, 479		Plate, rod	0.08[c]	2.0[c]	0.045[c]	0.03[c]	1.0[c]	16–18	10–14		2–3				
							Inconel Alloy 718								
C55445	8,9	25.2-mm pancake	0.05	0.21		0.006	0.05	18.18	52.16	0.06	3.03	b	b	5.31	0.76
GE Spec C50T79			0.10[c]	0.35[c]		0.03[c]	0.4[c]	17.0–21.0	50.0–55.0	0.75[c]	2.80–3.30			5.0–5.5	0.65–1.15

[a] All analyses include balance iron. No analysis available on Inconel alloy 718 heat Y8509 (Ref. 8). 2 1/4 Cr-1 Mo data used included bar and pipe forms conforming to the following specifications: 2.00–2.50% Cr; 0.9–1.1% Mo; room-temperature 0.2% offset yield strength ≥207 MPa (30 ksi); room-temperature ultimate tensile strength ≥414 MPa (60 ksi), reported in Ref. 10.

[b] Not reported.

[c] Maximum allowed.

Table 2. Heat Treatments and Specimen Gage Lengths of Materials Studied

Heat, Description	Initial Gage Length (mm)	Treatment	Time (hr)	Temperature (°C)	Cooling Method
		Type 304 Stainless Steel			
9T2796, 25-mm plate	57.2[a]	Anneal	0.5	1093	Air cool
9T2796, 51-mm plate	57.2	Anneal	0.5	1093	Air cool
8043813	57.2[a]	Anneal	0.5	1065	Air cool
55697	31.8	Anneal	1.0	1066	Rapid air cool
		Type 316 Stainless Steel			
332990	31.8	Anneal	1.0	1066	Rapid air cool
Garofalo et al.	38.1	Anneal	0.5	1093	Water quench
		2 1/4 Cr-1 Mo Steel			
Annealed[b]	50.8[c]	Austenitize	1	927	Furnace cool 28°C/hr to 450°C Air cool to room temperature
Isothermally annealed[b]	50.8[c]	Austenitize	1	927	Furnace cool 83°C/hr to 704°C
		Hold	2	704	Furnace cool 333°C/hr to room temperature
		Inconel Alloy 718			
C56445	50.8	Anneal	2.0	982	Air cool
		Age	8.0	718	Furnace cool 55°C/hr to 621°C
		Age	8.0	621	Air cool
Y8509	Unknown	Anneal	1.0	982	Water quench
		Age	8.0	718	Furnace cool 11–56°C/hr to 621°C, air cool

[a]Some high-stress and/or low-temperature tests were run on 31.8-mm-gage-length specimens.

[b]Typical heat treatment.

[c]Some tests were run on 76.2-mm-gage-length specimens.

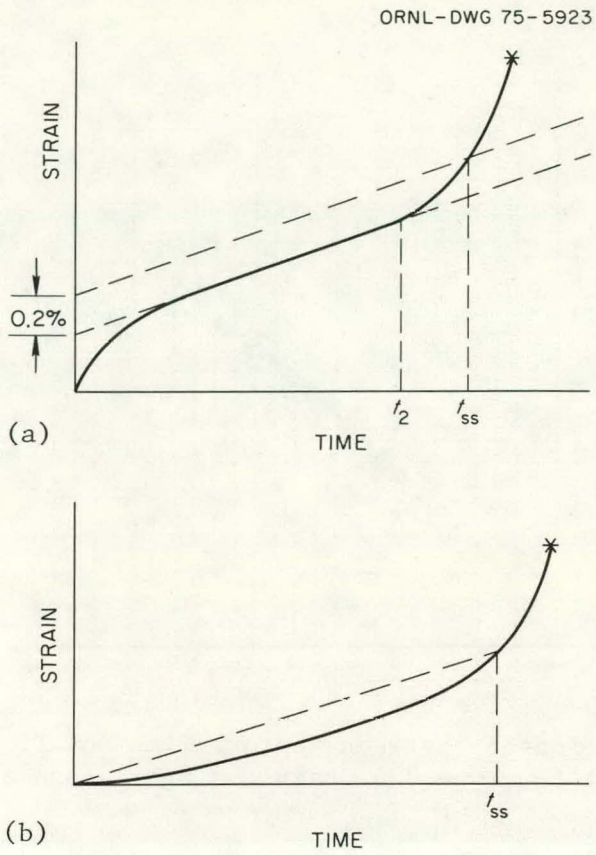

Fig. 1. (a) Definition of the Quantities t_2 and t_{ss} for a Classical Creep Curve. (b) Definition of t_{ss} for a common type of nonclassical creep curve.

the relationship between t_3 and the rupture life, t_r, may still be possible to determine since this relationship is simpler, given[12] by

$$t_3 = A t_r^{\beta} , \tag{1}$$

where A and β are material constants and are relatively independent of temperature and stress. Booker et al.[10] for instance, present an analysis of data for 2 1/4 Cr-1 Mo steel, wherein Eq. (1) yielded superior results to direct analysis of t_3 as a function of stress (σ) and temperature (T).

Figures 2 through 5 illustrate the results of analysis of data by Eq. (1), while Table 3 shows the values[10,12] of A and β along with some statistical information for the various data sets used. The results obtained by assuming A and β to be independent of temperature are quite good. However, to obtain maximum accuracy in predictions based on Eq. (1), this point must be considered in more detail.

The appendix discusses methods of statistical testing by which equations such as Eq. (1) and various others presented later in this report can be checked for dependence on temperature, heat-to-heat

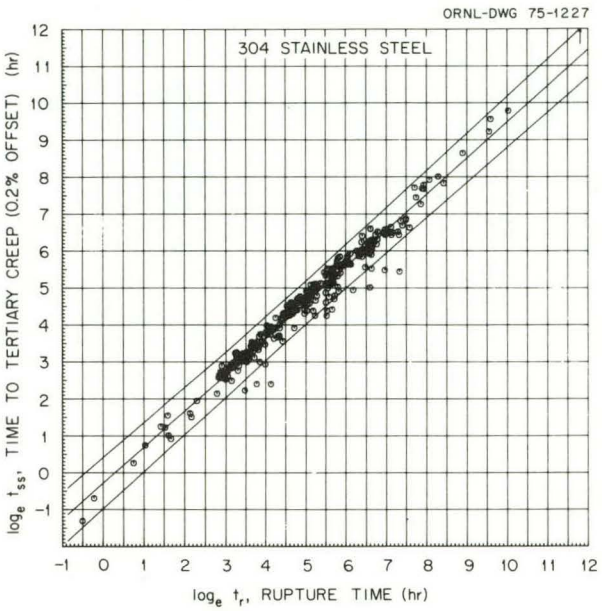

Fig. 2. Relationship Between Rupture Time and Time to Tertiary Creep (0.2% Offset) for Type 304 Stainless Steel (Annealed).

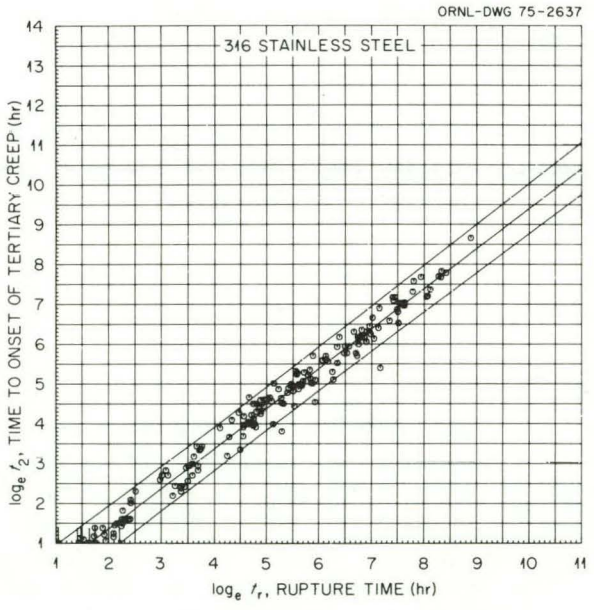

Fig. 3. Relationship Between Rupture Time and Time to Tertiary Creep for Type 316 Stainless Steel (Annealed).

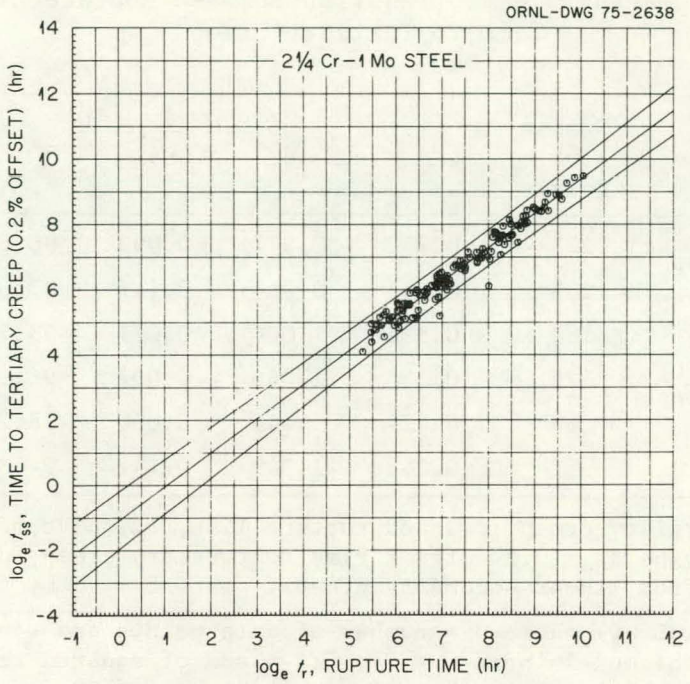

Fig. 4. Relationship Between Rupture Time and Time to Tertiary Creep (0.2% Offset) for 2 1/4 Cr-1 Mo Steel (Annealed and Isothermally Annealed).

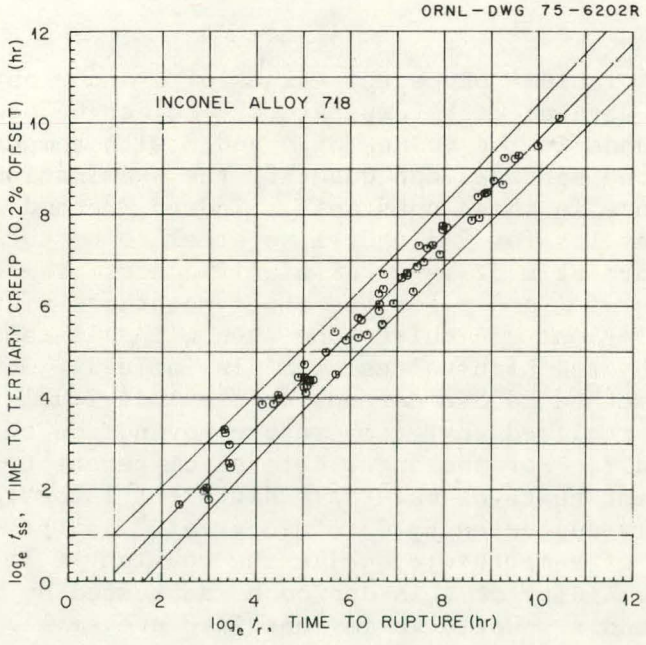

Fig. 5. Relationship Between Rupture Life and Time to Tertiary Creep (0.2% Offset) for Inconel Alloy 718 (Aged and Duplex Aged).

Table 3. Results of Correlation Between Rupture Life and Time to Tertiary Creep[a]

Data Set	Number of Points	A	β	RMS[b]	R^2[c]	Temperature Range of Data (°C)
304 Stainless, t_{ss}	277	0.752	0.977	0.090	96.6	482–816
304 Stainless, t_2	233	0.685	0.968	0.117	93.6	538–649
316 Stainless, t_2	183	0.526	1.004	0.071	93.5	538–816
2 1/4 Cr-1 Mo, t_{ss}	126	0.334	1.046	0.067	96.1	482–677
Inconel 718, t_{ss}	63	0.424	1.045	0.080	98.2	538–704
Inconel 718, t_2	52	0.285	1.049	0.142	94.3	538–704

[a] Time to tertiary creep, t_3, and rupture life, t_r, have been related by $t_3 = At_r^{\beta}$; t_3 may be t_{ss} (0.2% offset time to tertiary creep) or t_2 (time to first deviation from linear secondary creep).

[b] RMS = $\Sigma Y^2/(n - \nu)$ where n = number of data points and ν = number of coefficients in the model (here $\nu = 2$); ΣY^2 = sum of squared residuals, $\Sigma Y^2 = \Sigma(\ln t_{3_{pred}} - \ln t_{3_{exp}})^2$ where $\ln t_{3_{pred}}$ = ln [predicted rate (%/hr)] and $\ln t_{3_{exp}}$ = ln [experimentally observed rate (%/hr)].

[c] R^2 = coefficient of determination; R^2 describes how well a regression model describes variations in the data. $R^2 = 100$ signifies complete description, $R^2 = 0.0$ signifies no description. $\sqrt{R^2/100} = r$, the linear correlation coefficient.

variations, etc. Table 4 shows the values of A and β obtained by separate analysis of data at each temperature. As can be seen, there are no consistent trends in the values of A and β with temperature. Tests as described in the appendix can quantify the examination of the temperature dependence in these constants. Indeed, method A of the appendix found only the results for 2 1/4 Cr-1 Mo steel to be totally independent of temperature at a 5% level of significance. Therefore, use of isothermal values of A and β for the other materials might be justified. Still, the correlations are quite good even with all temperatures combined, as shown by the high values of R^2 in Table 3. Obviously the choice of which method to use depends on the individual situation. Also, it must be realized that temperature may not be the only factor influencing A and β. For instance, data at different temperatures may come from different heats of material, different laboratories, etc.

A possibility suggested by Garofalo et al.[6] is that the value of β is independent of temperature, while the constant A is temperature sensitive. The validity of this approach was tested by methods B, C, and D of the appendix. While variations in β are small, they are temperature sensitive to some extent.

Table 4. Results of Isothermal Correlation Between Rupture Life and Time to Tertiary Creep

Data Set	Temperature (°C)	Number of Points	A	β	RMS[a]	R^2
304 Stainless, t_{ss}	538	22	0.391	1.126	0.143	93.0
	593	174	0.994	0.942	0.031	98.4
	649	50	0.762	0.916	0.148	94.1
	704	14	0.447	1.053	0.034	99.5
	760	9	0.561	1.028	0.015	99.7
316 Stainless, t_2	538	8	0.665	1.011	0.068	98.0
	593	72	0.716	0.969	0.068	98.0
	649	12	0.594	0.905	0.104	98.2
	704	48	0.482	1.006	0.018	99.7
	760	7	0.260	1.109	0.031	99.3
	816	36	0.431	1.025	0.017	99.6
2 1/4 Cr-1 Mo, t_{ss}	538	24	0.282	1.050	0.123	91.6
	566	7	0.196	1.132	0.023	97.8
	593	46	0.266	1.078	0.049	97.2
	621	9	0.642	0.967	0.022	93.0
	649	29	0.317	1.057	0.060	96.8
	677	8	0.033	1.401	0.078	79.8
Inconel 718, t_{ss}	538	12	0.561	0.979	0.144	94.9
	593	10	0.439	0.989	0.292	94.0
	649	17	0.171	1.115	0.040	98.8
	704	13	0.171	1.107	0.149	93.6

[a] In terms of $\ln(t_3)$.

It should be noted that, if β were unity, Eq. (1) would reduce to the model form suggested by Leyda and Rowe:[17]

$$t_3 = F_s t_r \ , \qquad (2)$$

where F_s is a temperature-dependent constant. If the confidence intervals for β or the confidence ellipses for A, β (Appendix) contain 1 as a value for β, then Eq. (2) may be correct. However, since the regression constants A and β are merely estimates of the true values, it is preferable to use values obtained by least squares analysis. Setting β (or A) equal to any other value (e.g. β = 1) introduces an unnecessary bias in the results.

Parametric Analysis

The current data sets for both t_3 and t_r have been analyzed by use of standard time-temperature parameters.[12] In general, t_3 and t_r can be described by

$$t_3 = F(\sigma, T) \tag{3}$$

and

$$t_r = G(\sigma, T) , \tag{4}$$

where F and G are some functions of stress and temperature. Thus, we also have

$$t_3/t_r = F(\sigma, t)/G(\sigma, T) . \tag{5}$$

Equation (5) expresses the ratio of t_3 to t_r explicitly as a function of temperature and stress. Such an expression may lack some of the advantages of Eq. (1), since it cannot be determined unless sufficient data are available to perform parametric analyses for both t_3 and t_r. Still, Eq. (5) is useful, both for prediction of t_3 and for analysis of possible stress and temperature dependence of t_3/t_r. Equation (5) thus provides an interesting comparison with Eq. (1). Such comparisons have yielded similar results,[12] as illustrated in Fig. 6.

Stress-Based Correlations

A possible alternative to Eq. (1) might be to express σ_3, the stress to cause onset of tertiary creep in a given time at a given temperature, as a function of σ_r, the stress to cause rupture at the same time and temperature. Figure 7 illustrates results of such calculations for type 304 stainless steel obtained from the parametric results of Booker et al.[18] As seen in the figure, the correlation appears quite good. However, small variations in stress can cause relatively large variations in t_3 or t_r. Moreover, the construction of plots such as Fig. 7 requires the availability of enough data to calculate σ_3 and σ_r. These problems, coupled with the excellent correlations obtained by Eq. (1), tend to make time-based correlations more appealing.

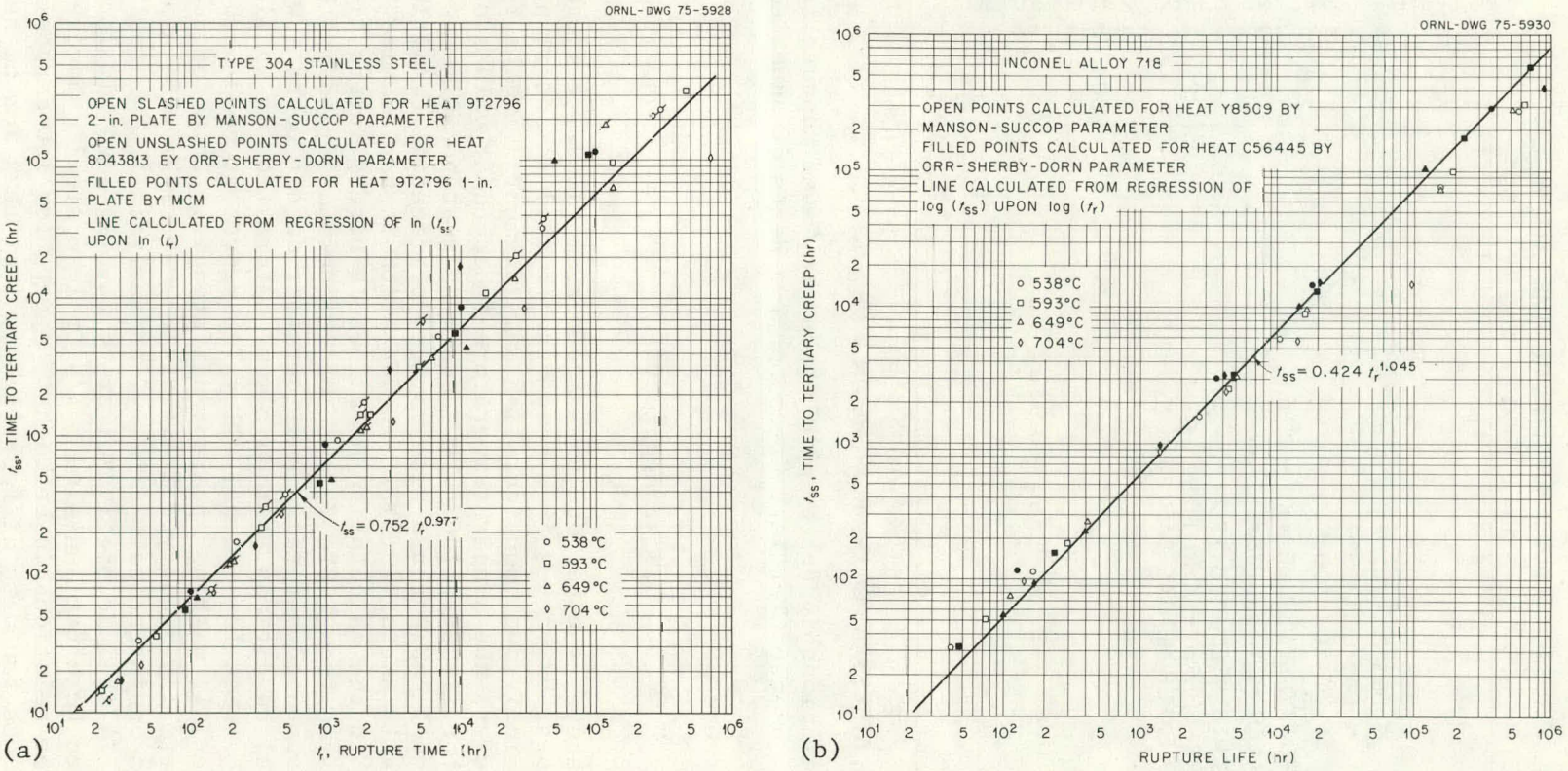

Fig. 6. Comparison Between Parametric Results for Single Heats and Relationship Between Rupture Time and Time to Tertiary Creep (0.2% Offset). (a) For type 304 stainless steel (annealed). (b) For Inconel alloy 718 (aged and duplex aged).

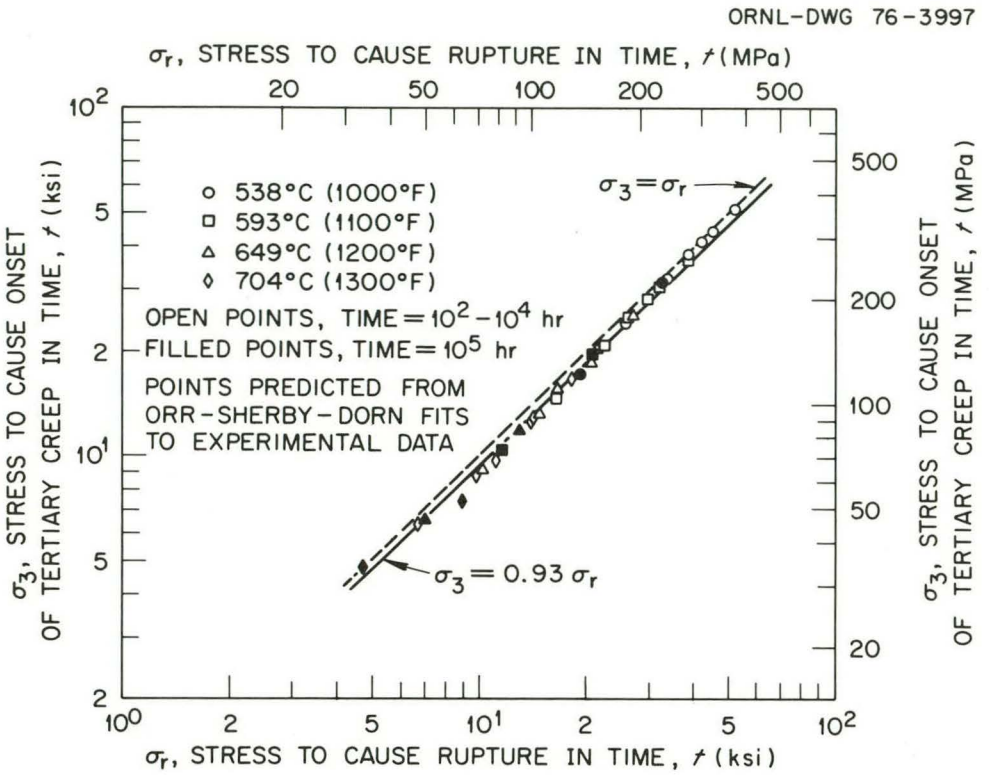

Fig. 7. Relationship Between the Stress to Cause Rupture and the Stress to Cause Onset of Tertiary Creep for Two Heats of Annealed Type 304 Stainless Steel.

Design Application

As stated above, whether one uses isothermal values, temperature-independent values, or values from some other method in actual practice is a matter for individual consideration and judgment. In the following discussion, however, the single temperature-independent values of A and β will be used for illustration. Two questions must be answered: (1) Is Eq. (1) applicable for a wide variety of material conditions and therefore generally useful? (2) If the equation is applicable, how can it best be used in the calculation of allowable stress intensities?

As can be seen from Table 2, most of the data analyzed in this report are for annealed material, and therefore do not cover a wide range of material conditions, although some information is available. For instance, the data for Inconel alloy 718 represent both aged and duplex aged material, with no apparent differences. Data for both annealed and thermally aged type 304 stainless steel have been presented[12] with again no inconsistencies. Finally, an analysis[19] of normalized and tempered 2 1/4 Cr-1 Mo steel similar to Eq. (1) gave similar results to those obtained here for annealed 2 1/4 Cr-1 Mo steel. However, in that analysis the relationship between t_3 and t_r for low-carbon (0.009–0.03%) material was found to differ slightly from that for higher carbon (0.12–0.135%) material. This possible dependence upon carbon content

could well be important, although it should be noted that both low-carbon heats from Ref. 19 fall below the minimum carbon content of 0.07% specified[20] for 2 1/4 Cr-1 Mo steel components in service above 371°C (700°F).

Heat-to-heat,[21] heat treatment, or other variations can be analyzed in exactly the same manner as were temperature variations above (Appendix). For example, three major data sets [heat 9T2796 25-mm (1-in.) plate, heat 9T2796 51-mm (2-in.) plate, and heat 8043813] are available for t_{ss} for type 304 stainless steel. These three sets can then be treated exactly as sets for three different temperatures would have been treated above. Figure 8 shows the data for the three individual heats separately and for all three combined, including best fit lines for Eq. (1). Analysis according to method A in the appendix, in fact, showed no significant variations among these three sets of data, although heat 8043813 is a relatively strong heat and 9T2796 is relatively weak. Thus, available information indicates that Eq. (1) is applicable over a range of conditions. The values of A and β may be influenced by variations in composition, heat treatment, processing history, etc., although there is little evidence to indicate this influence.

For use in setting allowable stresses one is interested in determining the minimum stress to cause onset of tertiary creep at a given time and temperature. To express t_3 as a function of stress and temperature, one must first express t_r (for which there are presumably sufficient data) as a function of stress and temperature, $F(\sigma, T)$; then Eq. (1) may be applied to this function. This procedure, of course, involves a double extrapolation and should therefore be performed with caution. Figure 9 illustrates the results obtainted by expressing t_3 as a function of stress and temperature by the procedure discussed above, where these results are shown to agree well with direct analysis of time to tertiary creep data using an Orr-Sherby-Dorn[22] time-temperature parameter for an individual heat of type 304 stainless steel. The real advantage of Eq. (1) is found in the analysis of multi-heat data sets such as might be required for determining allowable stresses. In this case, data scatter might make direct analysis difficult, whereas Eq.(1) could still be used since that relationship generally involves less scatter. Then, lower limit values can be calculated in various ways depending upon the situation. (It must be realized that the scatter in t_3 is real and cannot be reduced by any analytical technique. The current approach merely aids in identifying trends in the data.)

Probably, the most conservative approach to setting lower limits involves first determining a lower limit for t_r as a function of stress and temperature, $F'(\sigma, T)$; then a lower limit on Eq. (1) yields $t_3 = G'(t_r)$. The lower limit on t_3 is then $G'(F')$. This procedure was followed by Booker et al.[10] for 2 1/4 Cr-1 Mo steel (see Fig. 10). In some cases, it may be appropriate to use $t_3 = G'(F)$ as the lower limit, since the above method might yield overconservative results. At a given temperature, the stress that yields a value of $G' = t$ is the lower limit or "minimum" stress to cause onset of tertiary creep in time t.

To apply this approach, one must have a good method for setting lower limits on F and G. Hebble[16] addresses this problem in some detail; he found that the use of tolerance limits is generally the best approach.

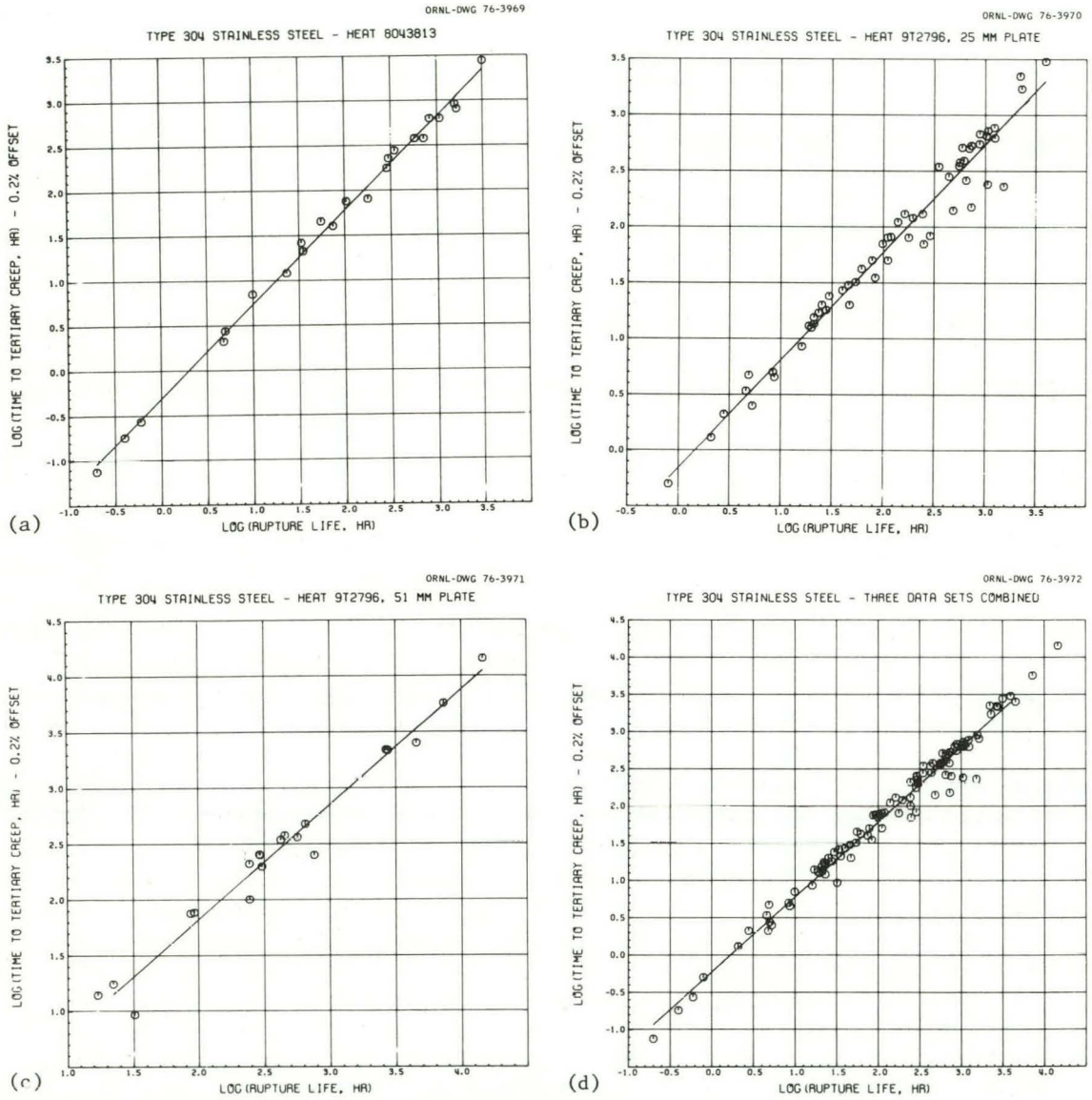

Fig. 8. Relationship Between Rupture Life and Time to the Onset of Tertiary Creep (0.2% Offset) for Type 304 Stainless Steel. (a) Heat 8043813; (b) heat 9T2796 25-mm (1-in.) plate; (c) heat 9T2796 51-mm (2-in.) plate; (d) all three combined.

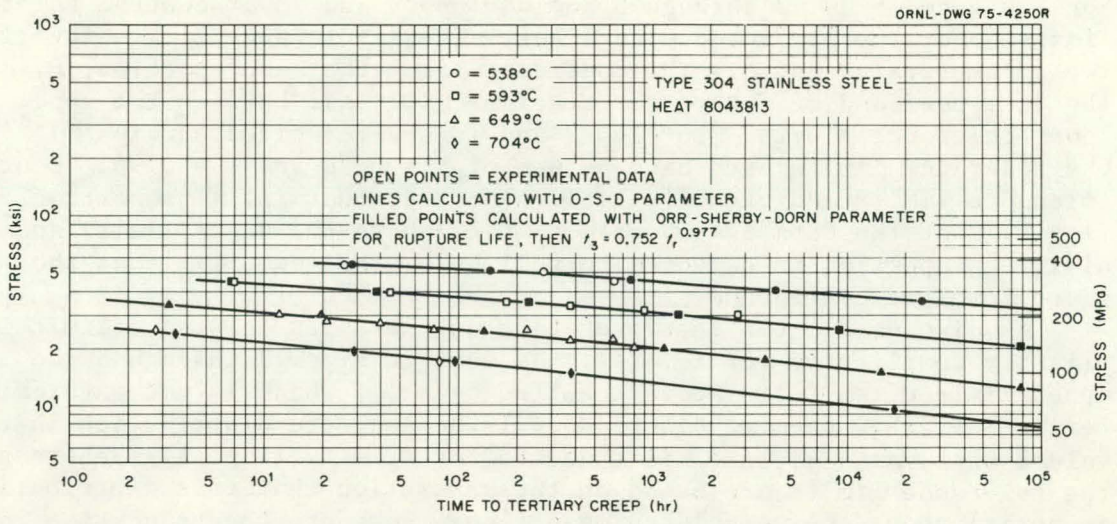

Fig. 9. Comparison of Predicted Time to Onset of Tertiary Creep (0.2%) with Experimental Data for Heat 8043813, Type 304 Stainless Steel. Also shown are direct parametric predictions from Ref. 18.

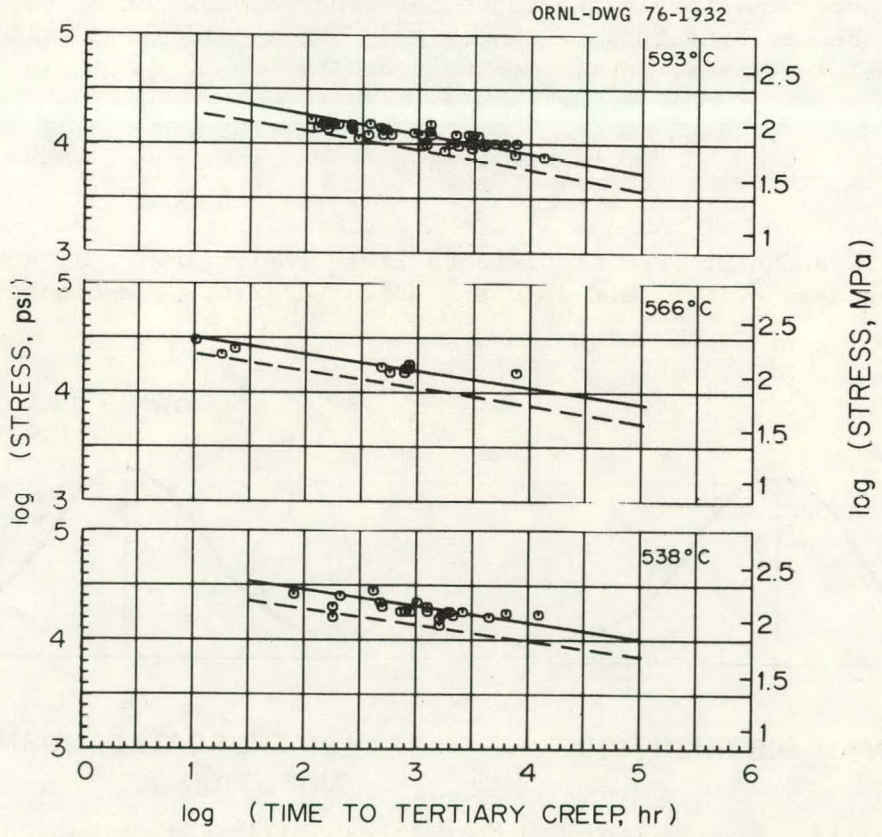

Fig. 10. Comparison of Predicted Time to Onset of Tertiary Creep (0.2%) with Experimental Data for 2 1/4 Cr-1 Mo Steel, Including Predicted Lower Limits.

For instance, Figs. 2 through 5 include upper and lower central tolerance limits about the predicted mean lines. These tolerance limits involve two parameters, P and λ. The confidence is λ that a proportion, P, of the data used and of future observations will fall between the upper and lower tolerance limits. In Fig. 2 and in several cited studies[10,12,16] the tolerance limits used have values of $P = 0.90$ and $\lambda = 0.95$. Central tolerance limits additionally imply symmetry; that is, a proportion $(1 - P)/2$ of the data is expected to fall above the upper limit, and a similar proportion is expected to fall below the lower limit at the given level of confidence.

As discussed[12] the interpretation of the upper tolerance limit is slightly complicated for Eq. (1). As seen in Figs. 2 through 5 the upper limit often falls above the line $t_3 = t_r$, which is not physically realistic. This seeming discrepancy is because the distribution in the values of t_3 at a given t_r is truncated at $t_3 = t_r$ (Fig. 11), whereas the tolerance limits are based on the assumption that this distribution is normal about the calculated mean line. However, the truncation in the actual data is not abrupt, and the assumption of normality has been found to be good by use of statistical testing methods.[23] Thus, the lower tolerance limits in Figs. 2 through 5 and Ref. 12 are still valid. For design use, of course, these lower limits are the properties of interest.

An approximation to the above tolerance limits can be obtained through the use of tolerance tables.[24] With a calculated value for $\ln t_3$, a lower limit, $\ln t_3'$ can be found by

$$\ln t_3' = \ln t_3 - Cs \ , \qquad (6)$$

where C is a factor from a tolerance table reflecting P, λ, and the number of data points, and s is the standard error of estimate for

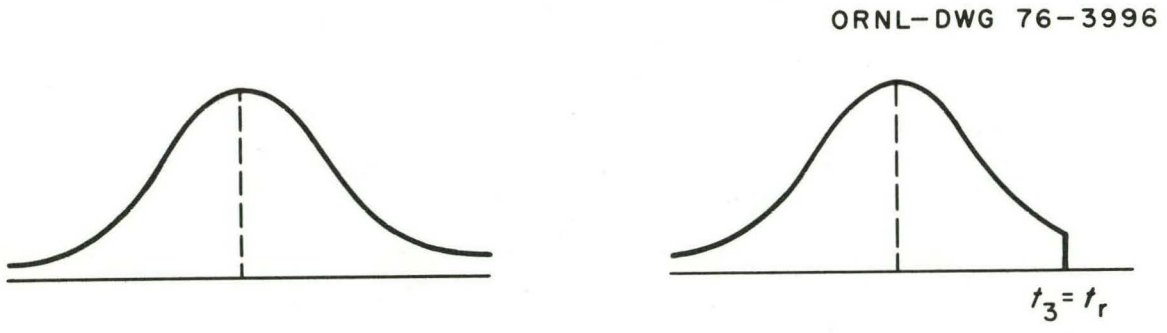

Fig. 11. Comparison of a Normal Possibility Distribution with a Truncated Distribution, which Illustrates the Distribution of $\log(t_3)$ as a Function of $\log(t_r)$.

ln t_3; $s = \sqrt{\text{RMS}}$ as given in Table 3. The above tolerance limits will yield larger safety factors in the extrapolated region, reflecting the larger uncertainties involved. These approximate tolerance limits, however, yield constant safety factors throughout, since they yield

$$t_3' = t_3 e^{-Cs} , \tag{7}$$

regardless of the value of t_3.

It should be noted that most "minimum" values[1] in ASME Code Case 1592 were calculated by a method somewhat similar to the above approximate tolerance limits, except that the code case limits are based on stress, the independent variable, since such a limit is then directly applicable to the setting of allowable stress levels. Also, the C value used is generally arbitrarily set at 1.65, which corresponds to the statistical value if the mean and standard deviation are known exactly.

RELATIONSHIPS BETWEEN RUPTURE LIFE AND MINIMUM CREEP RATE

One of the most widely known and used empirical relationships between creep properties is the relationship between minimum creep rate and rupture life proposed by Monkman and Grant,[25] which may be expressed as

$$\dot{e}_m = F t_r^{-\lambda} , \tag{8}$$

where, according to Monkman and Grant, F is a material constant that is independent of temperature and λ is a constant near unity. If λ is unity, Eq. (8) reduces to

$$\dot{e}_m t_r = F . \tag{9}$$

The quantity $\dot{e}_m t_r$ in Eq. (9) is Ivanova's[26,27] "plasticity resource," e_s. Several investigators[28,29] have discussed e_s as being a constant independent of stress and temperature, implying that Eq. (9) is indeed applicable. Others[19,30,31] have found that the relationship between $\dot{e}_m$ and t_r varies with temperature, although at a given temperature the general Monkman-Grant approach still applies.

Table 5 displays values of F and λ obtained in an analysis of the current data sets by Eq. (8) as discussed elsewhere.[31] Figure 12 illustrates the fits to experimental data from which the values in Table 5 were obtained. The R^2 values in the table show the fits to be excellent except for the 2 1/4 Cr-1 Mo steel data, for which the fit is somewhat inferior. These relatively poor fits can probably be explained from the results of Ref. 10, where for this material, the minimum creep

Table 5. Results of Correlation Between Rupture Life and Minimum Creep Rate

Data Set	Temperature (°C)	Number of Points	F	λ	RMS	R^2
304 Stainless	538	24	8.604	1.115	0.237	94.0
	593	41	15.991	1.180	0.214	96.4
	649	45	24.522	1.119	0.160	97.7
	704	14	28.633	1.086	0.140	98.2
	760	11	31.416	1.042	0.0339	99.5
316 Stainless	538	8	10.452	1.232	0.159	94.6
	593	48	6.410	0.982	0.0949	97.8
	649	12	21.574	1.000	0.0591	99.2
	704	48	32.259	1.038	0.0476	99.3
	760	7	29.207	1.003	0.0183	99.5
	816	36	35.696	1.082	0.0318	99.4
Inconel 718	538	8	13.296	1.378	0.162	98.5
	593	11	2.791	1.211	0.897	90.9
	649	13	1.393	1.142	0.362	95.5
	704	11	2.405	1.165	1.022	81.4
2 1/4 Cr-1 Mo	538	26	7.030	1.075	0.795	65.4
	593	45	97.820	1.414	0.751	81.5
	649	28	36.122	1.316	0.536	84.0

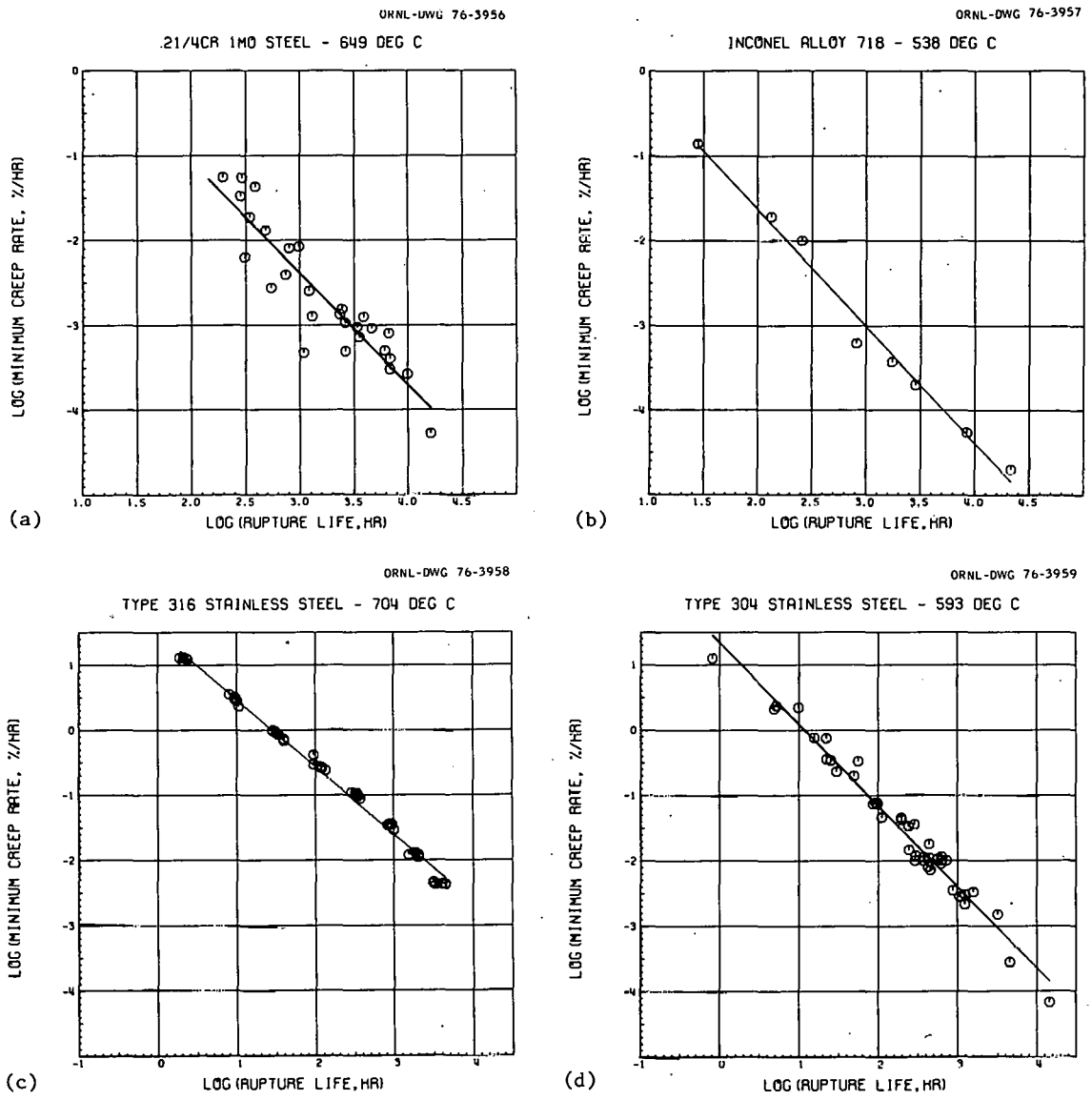

Fig. 12. Isothermal Relationship Between Minimum Creep Rate and Rupture Life. (a) 2 1/4 Cr-1 Mo steel at 649°C (1200°F). (b) Inconel alloy 718 at 538°C (1000°F). (c) Type 316 stainless steel at 704°C (1300°F). (d) Type 304 stainless steel at 593°C (1100°F).

rate was found to depend upon room-temperature ultimate tensile strength (τ), whereas the rupture life did not show such a dependence.

While the values of λ in Table 5 are indeed near unity, the values of F are apparently temperature sensitive. For the stainless steels, F generally increases with temperature; for the other materials consistent trends are less obvious but variations do appear to exist. Temperature dependence could be statistically checked by the same methods discussed in conjunction with Eq. (1) earlier, as outlined in the appendix. Although the variations of F and λ with temperature are not clearly systematic, this behavior is partially due to the effects of having two simultaneously varying constants.

Variations in F with temperature may be examined by letting λ be a constant and F be some analytical function of temperature. No extensive investigations of this type have been attempted, although all data have been examined by use of a simple expression of the form

$$\dot{e}_m = F_0 e^{-Q/RT} t_r^{-\lambda_0} , \tag{10}$$

where F_0, Q, and λ_0 are material constants that are independent of temperature, R is the gas constant (R = 8.31 J mole^{-1}K^{-1}), and T is the temperature in K. Results of correlations obtained using Eq. (10) are summarized in Table 6. As illustrated in Fig. 13, these correlations are indeed quite good, except again, in the case of 2 1/4 Cr-1 Mo steel. The Q values in Table 6 indicate that, at the given λ values, F increases with temperature for the stainless steels and decreases for the other two materials. Equation (10) thus allows calculation of $\dot{e}_m$ as a continuous function of T and t_r.

Table 6. Results of Correlation Among Minimum Creep Rate, Rupture Life, and Temperature[a]

Data Set	Temperature Range of Data (°C)	Number of Points	F_0	Q	λ_0	RMS[b]	R^2[c]
304 Stainless	482–816	144	56,552	60,768	1.133	0.0424	97.3
316 Stainless	538–760	159	15,999	593.84	1.020	0.0344	97.0
Inconel 718	538–760	46	0.324	−16,592	1.215	0.119	91.5
2 1/4 Cr-1 Mo	454–677	128	0.229	−34,932	1.280	0.179	73.1

[a]Minimum creep rate, $\dot{e}_m$, has been expressed as a function of rupture life, t_r, and temperature (K), T, by $\dot{e}_m = F_0 e^{-Q/RT} t_r^{-\lambda_0}$, where R is the gas constant, 8.31 J mole^{-1}K^{-1}.

[b]RMS expressed in terms of $\log(\dot{e}_m)$.

[c]Coefficient of determination.

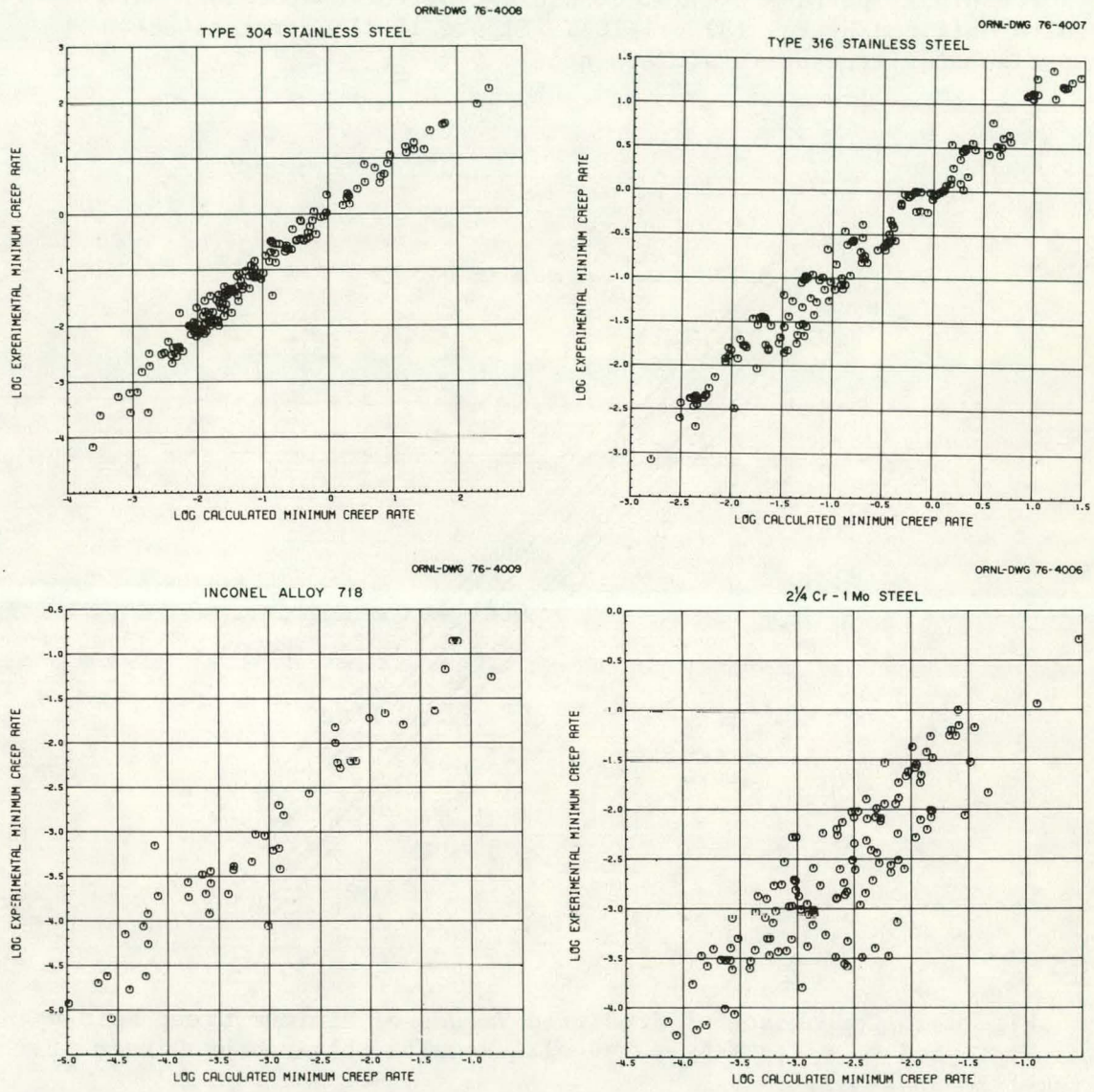

Fig. 13. Comparison of Predicted Values of Minimum Creep Rate With Experimental Values; $\dot{e}_m(\text{calc}) = F_0 e^{-Q/RT} t_r^{-\lambda_0}$.

Parametric Analysis

The relationship between t_r and $\dot{e}_m$ can be examined by a separate analysis of each as a function of stress and temperature in exactly the same manner used earlier in this report for t_r and t_3. Again, such a relationship is perhaps of limited use except for comparisons with results obtained by Eq. (8) or (10). Figure 14 illustrates such a comparison for type 304 stainless steel.

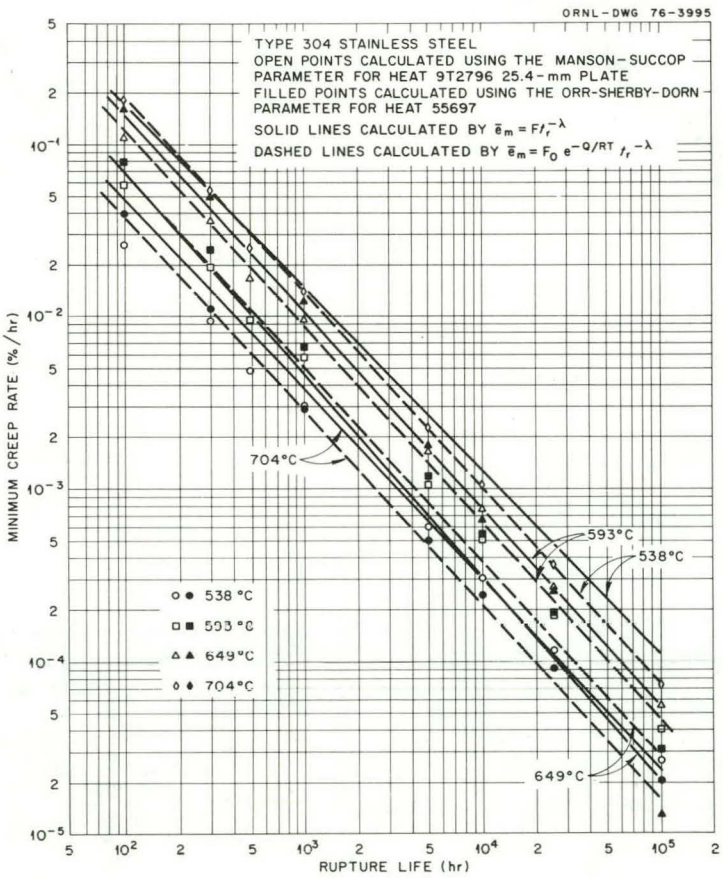

Fig. 14. Comparison of Predicted Values of Minimum Creep Rate by $\dot{e}_m = Ft_r^{-\lambda}$ and $\dot{e}_m = F_0 e^{-Q/RT}\ t_r^{-\lambda_0}$ with Results Obtained by Direct Parametric Analysis.

Stress-Based Correlations

Analogous to the stress-based correlations between σ_r and σ_3 mentioned above, σ_r can also be related to σ_m, the stress to cause a minimum creep rate of $1/t$ %/hr. Figure 15 shows such a correlation for type 316 stainless steel. The correlation is reasonably good but raises the same objections mentioned above for the σ_3-σ_r correlation.

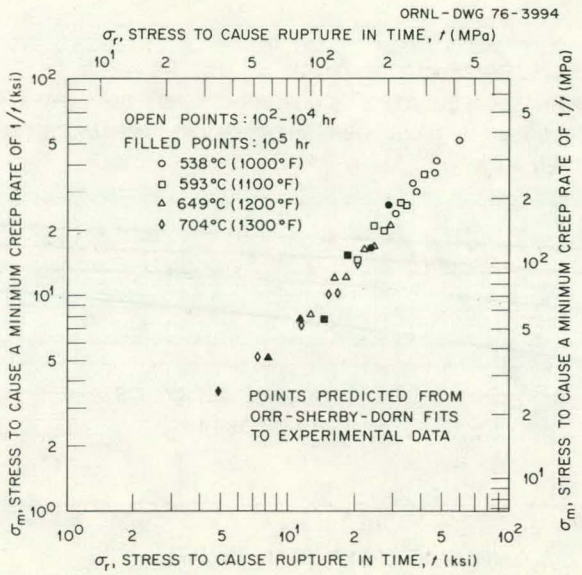

Fig. 15. Relationship Between the Stress to Cause Rupture in Time t and the Stress to Cause a Minimum Creep Rate of 1% in Time t for two Heats of Type 316 Stainless Steel.

Design Application

While the minimum creep rate is not itself an elevated-temperature design criterion, it can yield valuable information about the creep flow characteristics of a material. Also, a knowledge of $\dot{e}_m$ can be important in predicting the stress to 1% strain, as discussed later in this report. Use of Eq. (8) or (10) to predict the minimum creep rate has two main advantages over direct analysis of minimum creep rate as a function of stress and temperature. First, more rupture data are available, and thus t_r is better characterized than $\dot{e}_m$. Second, except for the 2 1/4 Cr-1 Mo steel, Eqs. (8) and (10) appear relatively independent of the heat-to-heat and other variations that complicate direct analysis. Figure 16 illustrates fits to actual experimental data using Eq. (10). Minimum values of $\dot{e}_m$ may be calculated by procedures analogous to those described earlier for t_3.

DUCTILITY PREDICTION

From Eq. (8), the plasticity resource, e_s, may be expressed at a given temperature as

$$e_s = F t_r^{1-\lambda} \tag{11}$$

or from Eq. (10) as

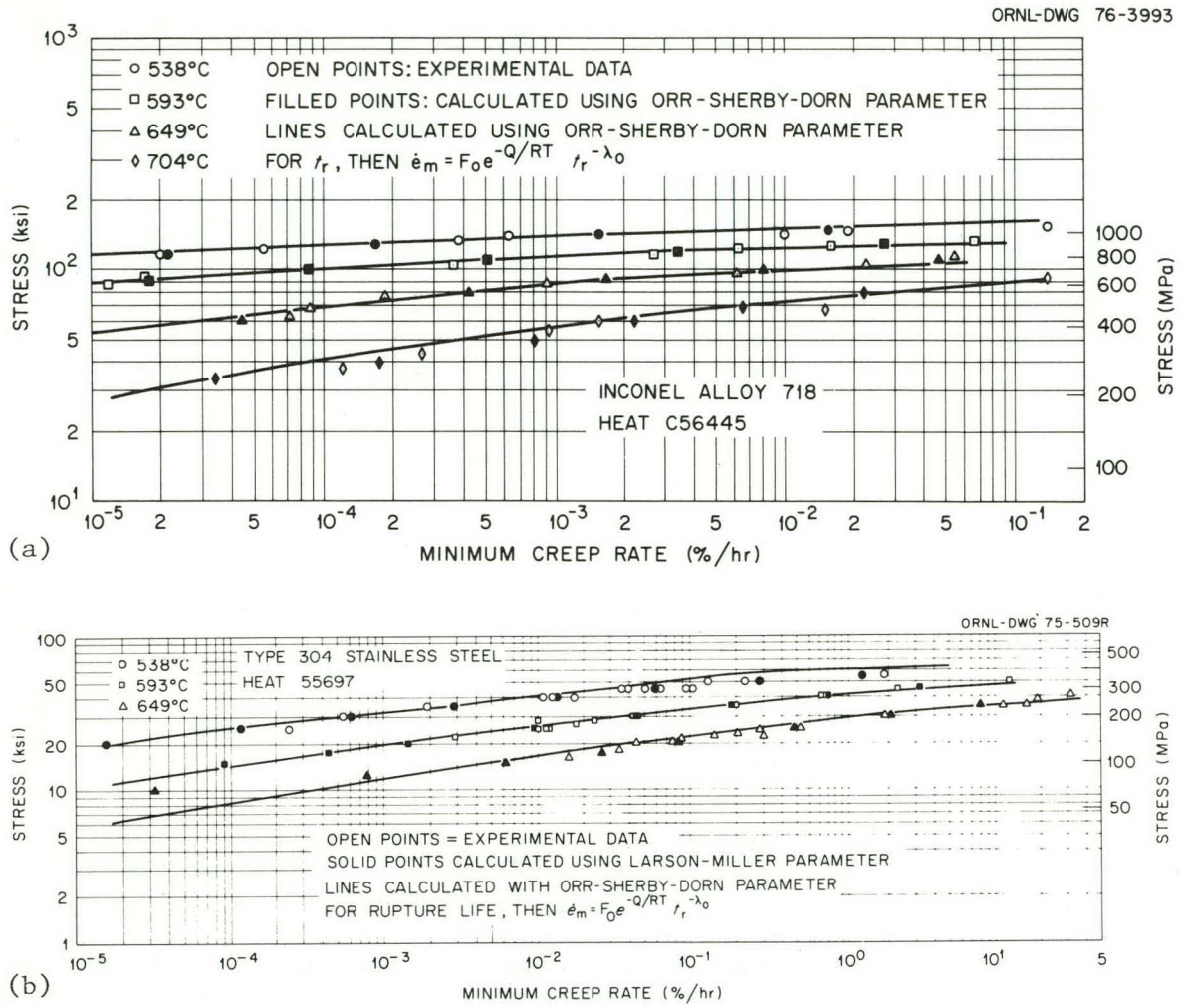

Fig. 16. Comparison of Predicted Values of Minimum Creep Rate ($\dot{e}_m = F_0 e^{-Q/RT}\ t_r^{-\lambda_0}$) with Experimental Data for (a) Inconel Alloy 718, Heat C56445 and (b) Type 304 Stainless Steel, Heat 55697. Also shown are direct parametric predictions from Ref. 18.

$$e_s = F_0 e^{Q/RT}\ t_r^{1-\lambda_0} \ . \tag{12}$$

Thus, one immediately has some measure of material ductility as a function of rupture life, and so indirectly as a function of stress and temperature. In fact, Ivanova and Oding[26,27] present e_s as an approximation to e_3, the strain to the onset of tertiary creep, although Goldhoff[32] has disputed the validity of this approximation.

Referring to Fig. 17, by definition

$$\dot{e}_m = (e_3 - e_p)/t_3 \ , \tag{13}$$

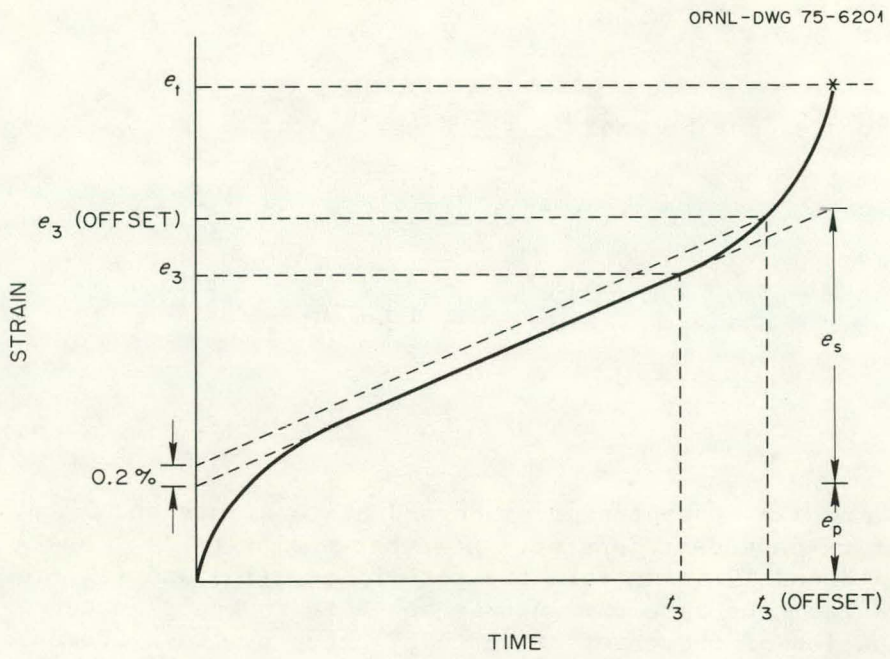

Fig. 17. Definition of Various Creep Properties Used.

so that

$$e_s = \dot{e}_m t_r = \frac{t_r}{t_3}(e_3 - e_p) \ . \tag{14}$$

Also, from Eq. (1)

$$t_r/t_3 = \frac{1}{A}\, t_r^{1-\beta} \ , \tag{15}$$

from which Eq. (14) becomes

$$e_s = \frac{1}{A}\, t_r^{1-\beta}\, (e_3 - e_p) \ . \tag{16}$$

Thus, the relationship between e_3 and e_s depends upon the primary creep behavior, although previous results[31] show that the two are reasonably close in magnitude.

The quantity e_3 is treated in Ref. 31 by methods similar to those used to develop Eq. (11) here. First, one defines $\dot{e}_3$, the average creep rate to tertiary creep, by

$$\dot{e}_3 = e_3/t_3 \quad . \tag{17}$$

As shown,[31] $\dot{e}_3$ may be empirically described by

$$\dot{e}_3 = B\dot{e}_m^{\alpha} \tag{18}$$

or

$$\dot{e}_3 = Dt_r^{-\gamma} \quad , \tag{19}$$

where B and α are temperature-independent constants and D and γ are temperature-dependent constants somewhat analogous to F and λ above. Figures 18 and 19 illustrate the fit of Eqs. (18) and (19) to experimental data. The same comments as above again apply concerning the determination of the onset of tertiary creep by two different methods. In addition, the data sets of Garofalo et al. on type 316 stainless steel and of heat Y8509 of Inconel alloy 718 listed in Table 1 include total strain; creep strain plus instantaneous strain incurred upon loading. The other data sets include creep strains only. Tables 7 and 8 summarize the results obtained by fitting Eqs. (18) and (19) to the current data sets.

As seen previously in Tables 5 and 6, the fits are excellent except for the 2 1/4 Cr-1 Mo steel. Table 8 shows the fit of Eq. (19) for this material to be relatively poor, again probably because for this material the flow properties (in this case $\dot{e}_3$) depend more upon initial strength than do the failure properties. Note, however, that the fit of Eq. (18) (Table 7), which relates two flow properties, is much better. The behavior of the constants D and γ is very similar to that of F and λ, discussed above. Thus, one might expect an equation analogous to Eq. (10) to be applicable.

Table 9 summarizes the correlations obtained by use of an equation of the form

$$\dot{e}_3 = D_0 e^{-Q/RT} t_r^{-\gamma_0} \quad , \tag{20}$$

where D_0, γ_0, and Q are temperature-independent material constants, R is the gas constant, and T is the temperature in K. As illustrated in Fig. 20, the fits are again quite good (except for the 2 1/4 Cr-1 Mo steel not shown), although not quite as good as those using Eq. (19) with isothermal values for D and γ.

Since $e_3 = \dot{e}_3 t_3$, Eqs. (1), (18), (19), and (20) allow e_3 to be expressed in any of three ways:

$$e_3 = AB t_r^{\beta} \dot{e}_m^{\alpha} \quad , \tag{21}$$

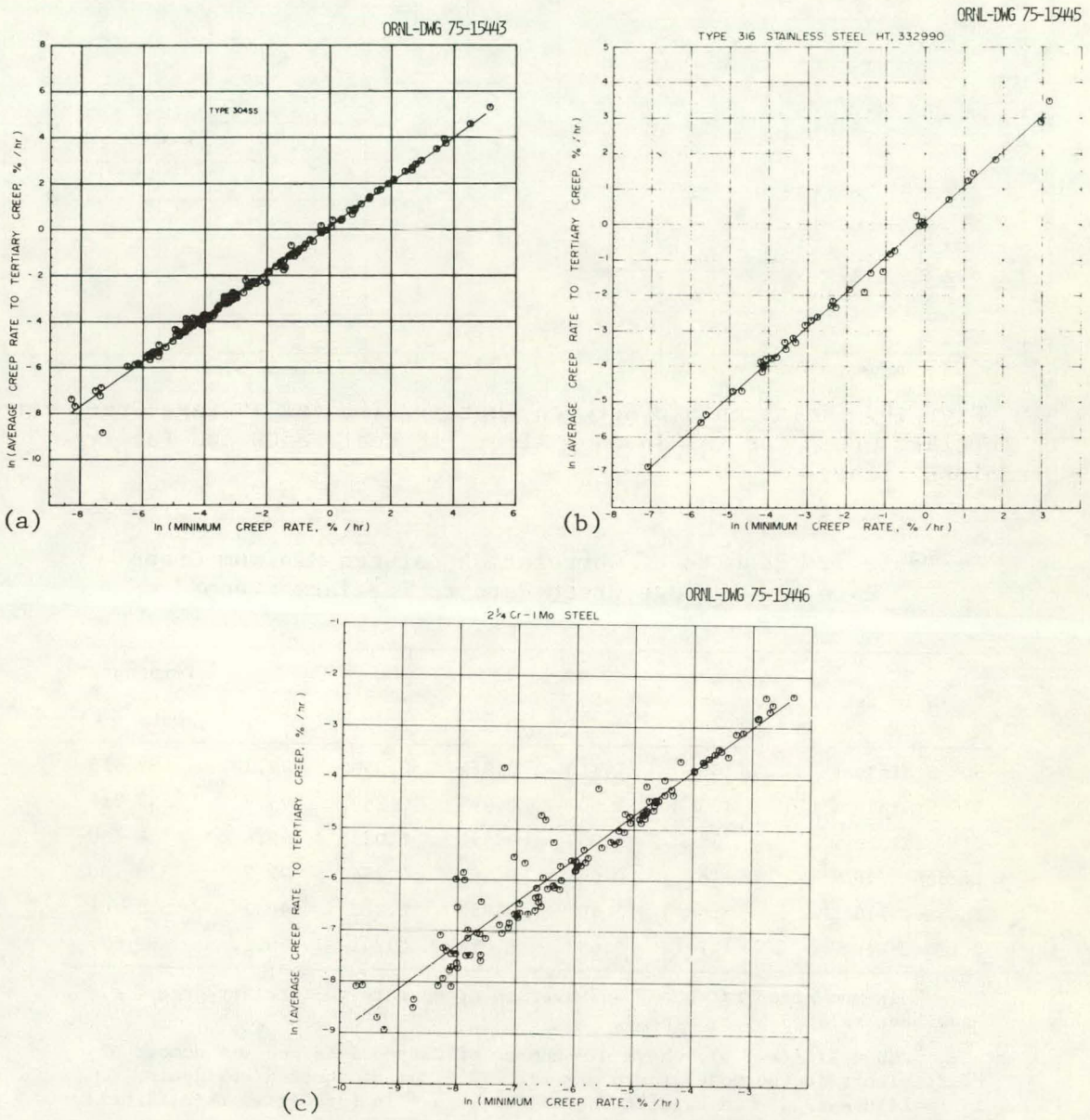

Fig. 18. Relationship Between Minimum Creep Rate and Average Creep Rate to Tertiary Creep for (a) Type 304 Stainless Steel, (b) Type 316 Stainless Steel Heat 332990, and (c) 2 1/4 Cr-1 Mo Steel.

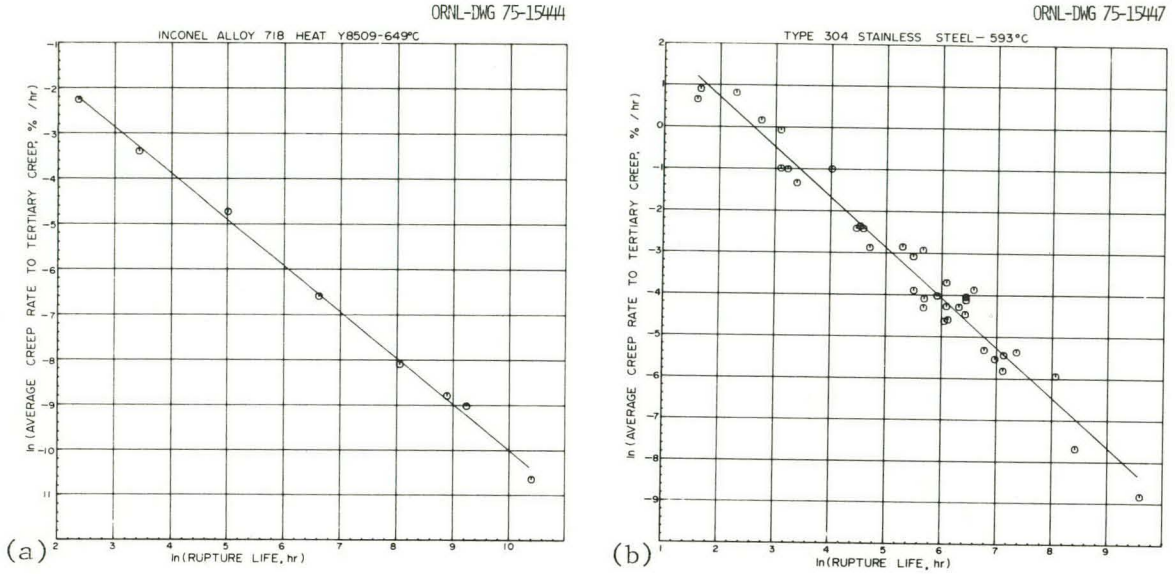

Fig. 19. Relationship Between Rupture Life and Average Creep Rate to Tertiary Creep for (a) Inconel Alloy 718 Heat Y8509 and (b) Type 304 Stainless Steel.

Table 7. Results of Correlation Between Minimum Creep Rate and Average Creep Rate to Tertiary Creep[a]

Data Set	Number of Points	B	α	RMS[b]	R^2[c]	Temperature Range of Data (°C)
304 Stainless	138	1.110	0.974	0.050	99.3	482–816
316 Stainless G[d]	120	1.602	0.995	0.269	95.6	593–816
316 Stainless H[e]	38	1.092	0.991	0.0235	99.6	538–760
Inconel 718 T[f]	18	0.684	0.86	0.254	92.2	538–760
Inconel 718 C[g]	26	1.40	0.985	0.322	96.2	538–704
2 1/4 Cr-1 Mo	117	0.637	0.854	0.241	90.2	482–677

[a] Minimum creep rate, $\dot{e}_m$, and average creep rate to tertiary creep, $\dot{e}_3$, have been related by $\dot{e}_3 = B\dot{e}_m^{\alpha}$.

[b] RMS = $\Sigma Y^2/(n - \nu)$, where n = number of data points and ν = number of coefficients in the model (here $\nu = 2$); ΣY^2 = sum of squared residuals, $\Sigma Y^2 = \Sigma(\ln \dot{e}_{3_{pred}} - \ln \dot{e}_{3_{exp}})^2$ where $\ln \dot{e}_{3_{pred}}$ = ln [predicted rate (%/hr)] and $\ln \dot{e}_{3_{eff}}$ = ln [experimentally observed rate (%/hr)].

[c] R^2 = coefficient of determination; R^2 describes how well a regression model describes variations in the data. $R^2 = 100$ signifies complete description, $R^2 = 0.0$ signifies no description. $\sqrt{R^2/100} = R$, the linear correlation coefficient.

[d] Data for total strain.

[e] Data for creep strain only.

[f] Data for total strain.

[g] Data for creep strain only.

Table 8. Results of Correlation Between Rupture Life and Average Creep Rate to Tertiary Creep[a]

Data Set	Temperature (°C)	Number of Points	D	γ	RMS[b]	R^2[c]
304 Stainless	538	24	4.899	1.030	0.174	94.4
	593	37	22.571	1.198	0.202	96.2
	649	44	25.091	1.089	0.172	97.3
	704	14	33.882	1.099	0.124	98.5
	760	11	33.115	1.034	0.048	99.3
316 Stainless G[d]	593	36	30.265	1.078	0.020	99.6
	704	48	49.383	1.081	0.030	99.6
	816	36	42.921	1.103	0.023	99.6
316 Stainless H[e]	538	7	7.131	1.154	0.174	93.5
	593	12	12.783	1.038	0.171	96.5
	649	12	23.220	1.005	0.027	99.6
	760	7	31.690	1.004	0.014	99.6
Inconel 718 T[f]	593	4	2.044	1.048	0.339	94.4
	649	6	27.859	1.442	0.121	97.4
	704	4	0.081	0.710	0.00406	99.5
	760	3	2.545	1.125	0.0566	97.0
Inconel 718 C[g]	538	6	32.394	1.429	0.491	97.0
	593	6	3.968	1.218	0.0636	99.3
	649	8	1.212	1.020	0.0259	99.7
	704	6	6.640	1.232	0.103	98.8
2 1/4 Cr-1 Mo	538	23	3.531	0.903	0.422	73.1
	593	41	51.761	1.280	0.699	77.2
	649	26	18.168	1.185	0.411	83.8

[a] Rupture life, t_r, and average creep rate to tertiary creep, $\dot{e}_3$, are related by $\dot{e}_3 = Dt_r^{-\gamma}$.

[b] RMS $= \Sigma Y^2/(n - \nu)$, where n = number of data points and ν = number of coefficients in the model (here $\nu = 2$); ΣY^2 = sum of squared residuals, $\Sigma Y^2 = \Sigma(\ln \dot{e}_{3pred} - \ln \dot{e}_{3exp})^2$ where $\ln \dot{e}_{3pred}$ = ln [predicted rate (%/hr)] and $\ln \dot{e}_{3exp}$ = ln [experimentally observed rate (%/hr)].

[c] R^2 = coefficent of determination; R^2 describes how well a regression model describes variations in the data. $R^2 = 100$ signifies complete description, $R^2 = 0.0$ signifies no description. $\sqrt{R^2/100} = r$, the linear correlation coefficient.

[d] Data for total strain.

[e] Data for creep strain only.

[f] Data for total strain.

[g] Data for creep strain only.

Table 9. Results of Correlation Among Average Creep Rate to Tertiary Creep, Rupture Life, and Temperature[a]

Data Set	Number of Points	D_0	Q	γ_0	RMS[b]	R^2 (%)[c]	Temperature Range of Data (°C)
304 Stainless	139	41,725	58,809	1.088	0.0380	97.3	482–816
316 Stainless G	120	132.7	10,063	1.072	0.00996	99.1	593–816
316 Stainless H	38	205,447	70,358	1.064	0.0341	97.1	538–760
Inconel 718 T	18	0.157	−27,037	1.226	0.0394	94.0	538–760
Inconel 718 C	26	2.99	−743	1.150	0.0378	97.6	538–704
2 1/4 Cr-1 Mo	115	0.07	−42,401	1.196	0.132	71.9	482–677

[a]Average creep rate to tertiary creep, $\dot{e}_3$, has been expressed as a function of rupture life, t_r, and temperature (K), T, by $\dot{e}_3 = D_0 e^{-Q/RT} t_r^{-\gamma_0}$, where R is the gas constant, 8.31 J mole^{-1}K^{-1}.

[b]RMS expressed in terms of $\log(\dot{e}_3)$.

[c]Coefficient of determination.

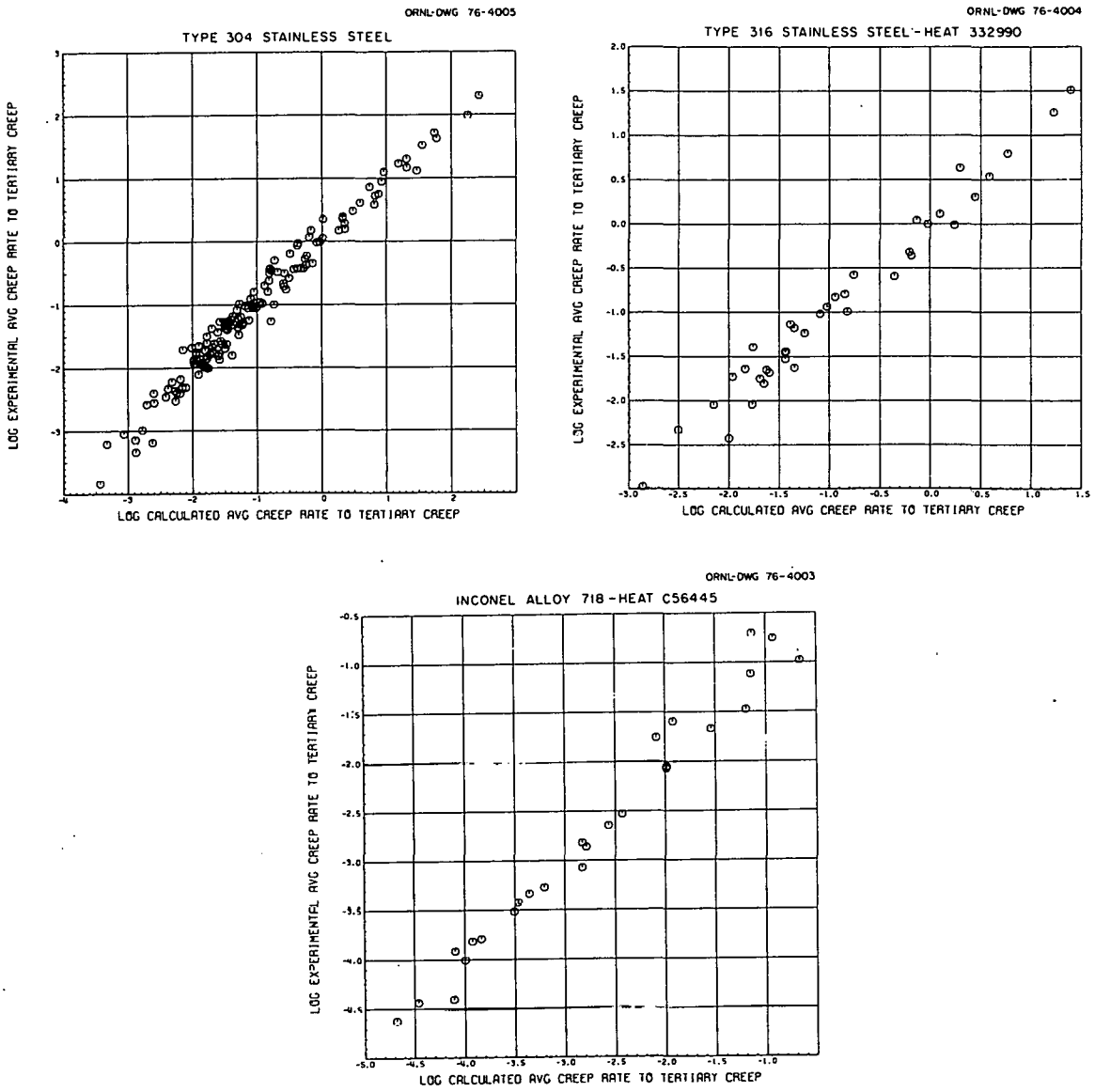

Fig. 20. Comparison of Predicted Values of Average Creep Rate to Tertiary Creep ($\dot{e}_3 = D_0 e^{-Q/RT} t_r^{-Y_0}$) with Experimental Values.

$$e_3 = AD t_r^{(\beta-\gamma)} \quad \text{(isothermally)} , \tag{22}$$

or

$$e_3 = AD_0 e^{-Q/RT} t_r^{(\beta-\gamma_0)} . \tag{23}$$

The treatment given e_s and e_3 here immediately suggests that the total creep strain (total strain for the Garofalo and Y8509 heats) to rupture, e_r, may be treated similarly. Analogous to the equations for e_3, one defines the average creep rate to rupture by

$$\dot{e}_r = e_r / t_r . \tag{24}$$

Then, one has

$$\dot{e}_r = C \dot{e}_m^{\rho} , \tag{25}$$

$$\dot{e}_r = E t_r^{-\delta} \quad \text{(isothermally)} , \tag{26}$$

$$\dot{e}_r = E_0 e^{-Q/RT} t_r^{-\delta_0} , \tag{27}$$

$$e_r = C \dot{e}_m^{\rho} t_r , \tag{28}$$

$$e_r = E t_r^{1-\delta} \quad \text{(isothermally)} \tag{29}$$

$$e_r = E_0 e^{-Q/RT} t_r^{1-\delta_0} . \tag{30}$$

It should be noted that e_r depends upon the elongation in the tertiary stage, which can include necking and other instabilities. Thus, the value of e_r is expected to be a function of specimen geometry, although the current data were insufficient to quantitatively determine such effects.[18]

Tables 10 through 12 and Figs. 21 through 23 demonstrate that Eqs. (25) through (27) are indeed applicable with very much the same results as those obtained above with Eqs. (18) through (20). However, since e_r is, like t_r, a rupture property, the results for the 2 1/4 Cr-1 Mo steel are considerably improved in relation to the other materials over those for e_s and e_3.

Table 10. Results of Correlation Between Rupture Life and Average Creep Rate to Rupture[a]

Data Set	Temperature (°C)	Number of Points	E	δ	RMS[b]	R^2 [c]
304 Stainless	538	24	66.67	1.225	0.098	97.7
	593	40	43.26	1.165	0.095	98.3
	649	45	46.41	1.103	0.130	98.0
	704	14	61.98	1.139	0.140	98.4
	760	11	52.28	1.081	0.100	98.7
316 Stainless C	593	36	11.64	1.022	0.127	97.3
	704	48	85.73	1.030	0.099	98.6
	816	48	127.29	1.151	0.031	99.6
316 Stainless H	538	8	121.04	1.292	0.026	99.2
	593	11	39.34	1.087	0.051	99.1
	649	12	52.05	1.027	0.048	99.3
	760	6	81.05	1.042	0.0006	99.9
Inconel 718 T	593	5	1.30	0.763	0.084	92.6
	649	9	4.29	1.154	0.076	97.6
	704	5	7.34	0.844	0.086	89.0
Inconel 718 C	538	7	2.28	0.124	0.063	98.6
	593	7	3.28	0.954	0.009	99.7
	649	7	3.50	0.939	0.066	98.1
	704	7	8.79	0.978	0.066	96.9
2 1/4 Cr-1 Mo	538	29	143.45	1.151	0.086	95.6
	593	47	185.17	1.213	0.103	95.9
	649	27	147.16	1.198	0.128	94.9

[a]Average creep rate to rupture, $\dot{e}_r$, and rupture life, t_r, have been related by $\dot{e}_r = Et_r^{-\delta}$.

[b]RMS in terms of $\ln(\dot{e}_r)$.

[c]Coefficient of determination.

Table 11. Results of Correlation Between Minimum Creep Rate and Average Creep Rate to Rupture[a]

Data Set	Temperature Range of Data (°C)	Number of Points	C	δ	RMS[b]	R^2[c]
304 Stainless	482–816	142	2.20	0.927	0.251	96.4
316 Stainless G	593–816	120	3.18	1.026	0.044	99.3
316 Stainless H	538–760	37	2.52	0.899	0.290	94.8
Inconel 718 T	538–760	19	4.20	0.756	0.413	71.0
Inconel 718 C	538–704	27	1.71	0.813	0.062	94.5
2 1/4 Cr-1 Mo[d]	482–677	126	1.34	0.650	0.741	64.6

[a]Minimum creep rate, $\dot{e}_m$, and average creep rate to rupture, $\dot{e}_r$, have been related by $\dot{e}_r = C\dot{e}_m^{\rho}$.

[b]RMS in terms of $\ln(\dot{e}_r)$.

[c]Coefficient of determination.

[d]Data in this case represent *total* strain.

Table 12. Results of Correlation Among Average Creep Rate to Rupture, Rupture Life, and Temperature[a]

Data Set	Temperature Range of Data (°C)	Number of Points	E_0	Q	δ_0	RMS[b]	R^2[c]
304 Stainless	482–816	143	22,578	50,559	1.086	0.0232	98.2
316 Stainless G[d]	593–816	132	7,319	37,451	1.081	0.0349	97.4
316 Stainless H	538–760	37	1.061×10^6	79,776	1.029	0.0124	98.8
Inconel 718 T[d]	538–760	24	1.044×10^5	68,400	1.015	0.0410	94.9
Inconel 718 C	538–704	28	1,266	41,781	0.981	0.0237	98.0
2 1/4 Cr-1 Mo[d]	482–677	134	36.19	−7,757	1.139	0.0247	94.0

[a]Average creep rate to rupture, $\dot{e}_r$, has been expressed as a function of rupture life, t_r, and temperature (K), T, by $\dot{e}_r = E_0 e^{-Q/RT} t_r^{-\delta_0}$, where R is the gas constant, 8.31 J mole^{-1}K^{-1}.

[b]RMS expressed in terms of $\log(\dot{e}_r)$.

[c]Coefficient of determination.

[d]Data for total strain, creep + loading.

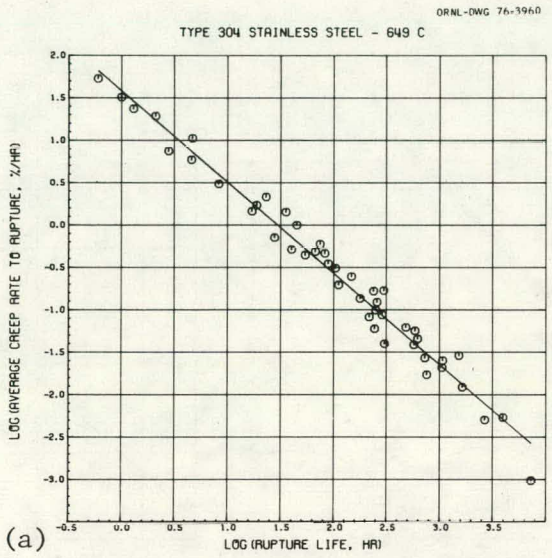

(a)

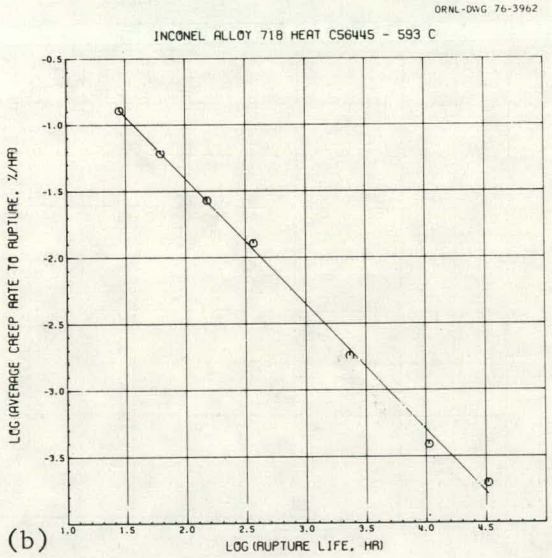

(b)

Fig. 21. Relationship Between Rupture Life and Average Creep Rate to Rupture for (a) Type 304 Stainless Steel at 649°C and (b) Inconel Alloy 718 Heat C56445 at 593°C.

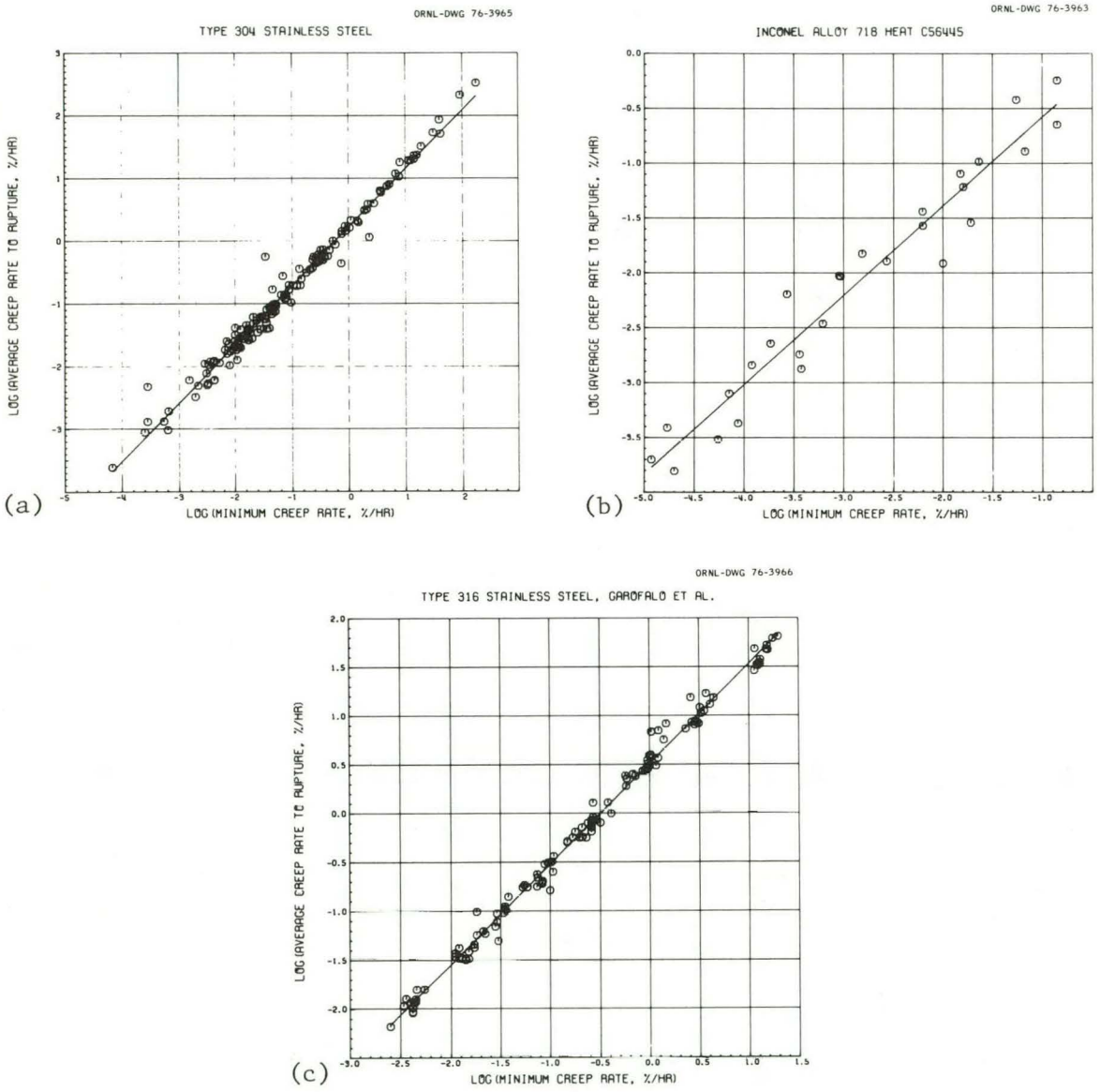

Fig. 22. Relationship Between Minimum Creep Rate and Average Creep to Rupture for (a) Type 304 Stainless Steel, (b) Inconel Alloy 718 Heat C56445, and (c) Type 316 Stainless Steel — Garofalo et al. Data Set.

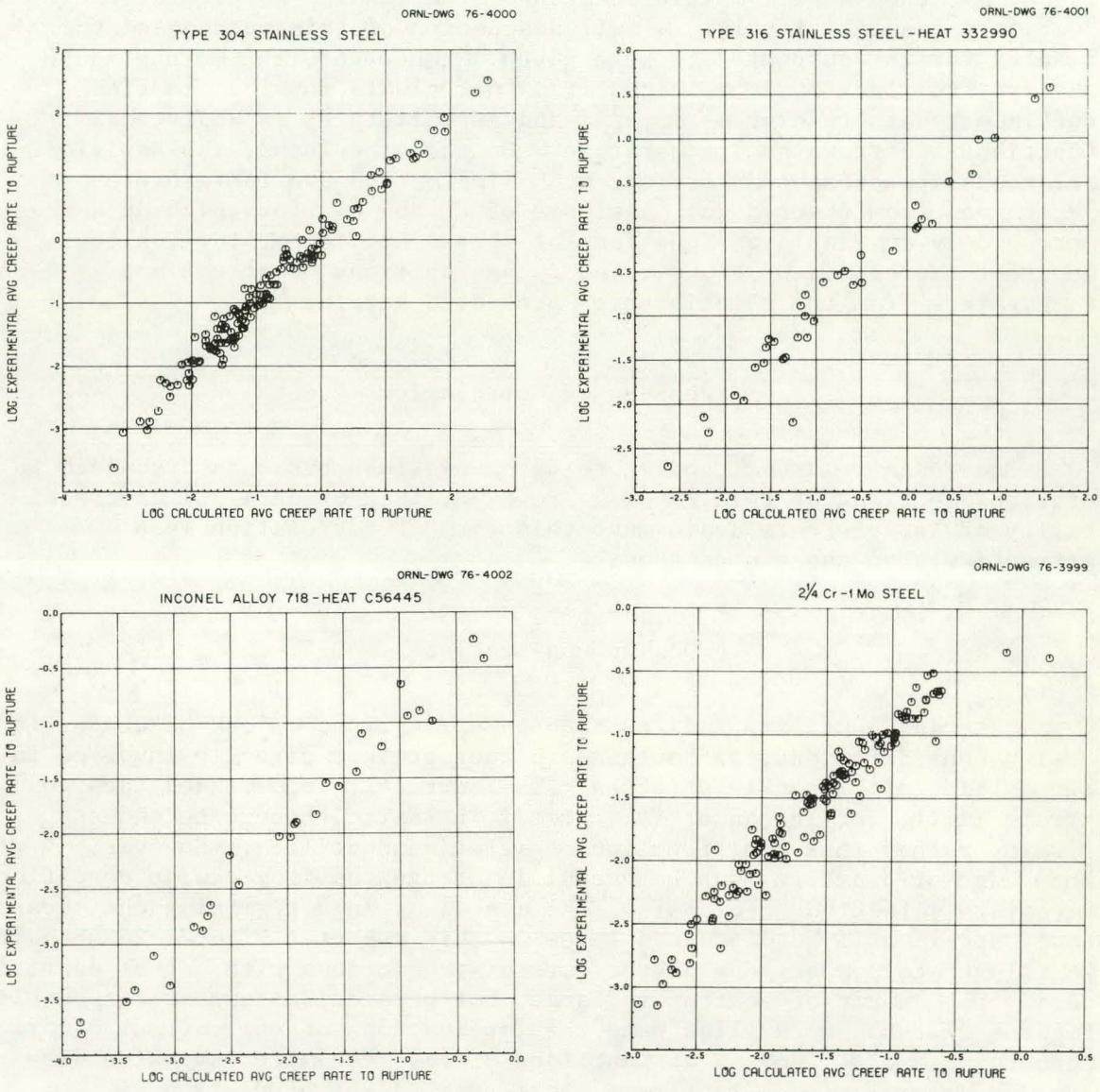

Fig. 23. Comparison of Predicted Values of Average Creep Rate to Rupture ($\dot{e}_r = E_0 e^{-Q/RT} t_r^{-\delta_0}$) with Experimental Values.

Parametric Analysis

We previously presented[18] a parametric analysis of several ductility properties, including e_g, e_3, and e_r, as functions of stress and temperature. This method consists simply of separate analyses of, say, t_3 and $\dot{e}_3$, then a back-multiplication of the results to predict the ductility quantity itself. A full discussion of this method and the results for the current data were given.[18] However, the method again suffers from lack of data, since it is not always possible to find sufficient data to express $\dot{e}_m$, $\dot{e}_r$, and especially $\dot{e}_3$ as analytical functions of stress and temperature. On the other hand, the empirical relationships presented here are much simpler and can therefore be determined from fewer data. Analysis of t_r and $\dot{e}_m$, for which data are more widely available as functions of stress and temperature, allows indirect expression of e_g, e_3, and e_r as functions of stress and temperature from the relationships presented herein.

Stress-Based Correlations

One could relate $\dot{e}_3$ and $\dot{e}_r$ to t_r on a stress basis as discussed in previous sections of this report. However, lack of data and the possibility of large errors again make this form of correlation less attractive than those used above.

Design Application

Material ductility indices such as e_g, e_3, and e_r can be useful in design considerations, although again they are not directly involved in the setting of allowable stresses. The currently recommended[1] design strain limit, for instance, is 1% total inelastic through-thickness strain, rather than some function of material ductility. However, knowledge of ductility can be useful in setting optimum design conditions, materials selection, etc. Also, the use of e_3 in determining the stress to 1% strain will be discussed later in this report. Figures 24 through 26 illustrate comparisons of the current predictions with actual ductility data. The amount of scatter is large, but predictions appear reasonable. Figures 27 through 29 illustrate the implications of the current equations concerning e_g, e_3, and e_r as functions of t_r. Far more extensive discussion is presented elsewhere[18,31] concerning the prediction of ductility, including the calculation of lower limits. More extensive discussion of the uses of ductility in design can also be found in those references.

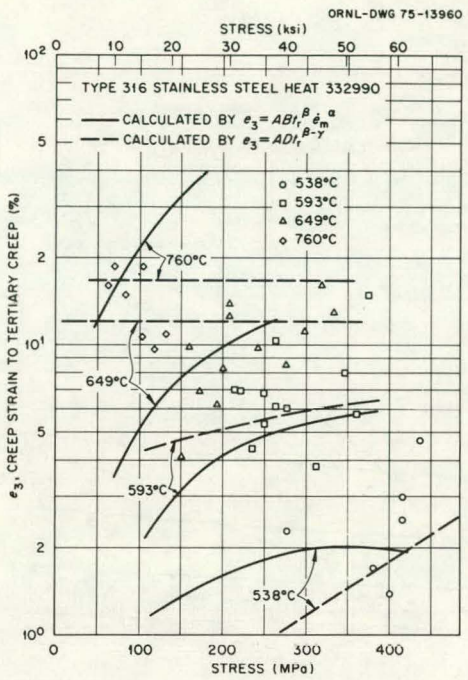

Fig. 24. Comparison of Predicted Values for Strain to Tertiary Creep ($e_3 = ADt_r^{\beta-\gamma}$) with Experimental Data for Type 316 Stainless Steel. Also shown are parametric predictions.[18]

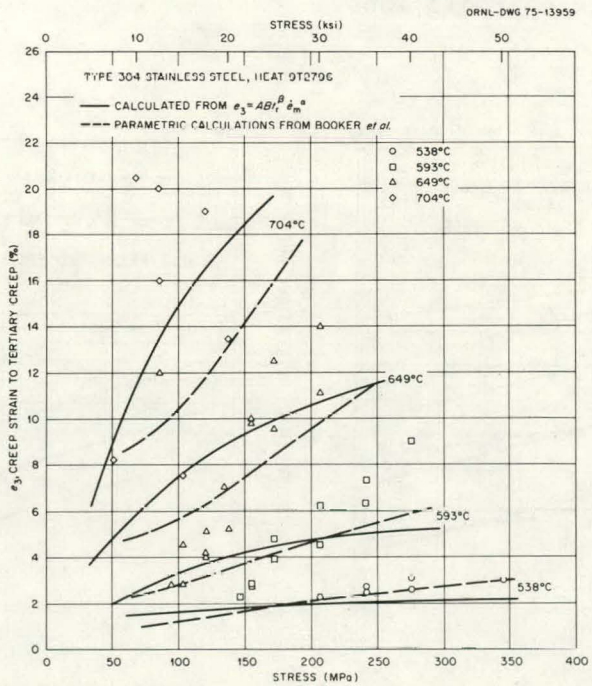

Fig. 25. Comparison of Predicted Values for Plasticity Resource ($e_s = Ft_r^{1-\lambda}$) with Experimental Data for Type 304 Stainless Steel, Heat 9T2796, 25-mm Plate. Also shown are parametric predictions.[18]

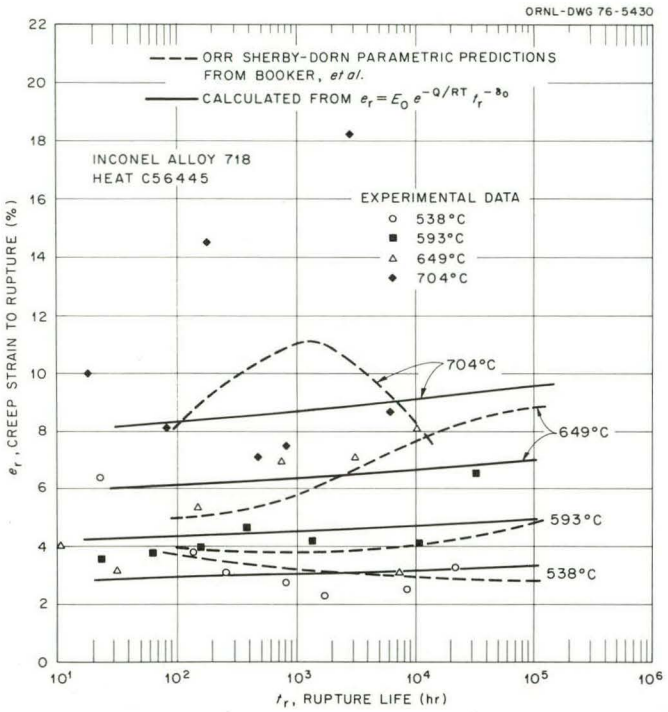

Fig. 26. Comparison of Predicted Values of Creep Strain to Rupture with Experimental Data for Inconel Alloy 718, Heat C56445. Also shown are direct parametric predictions.[18]

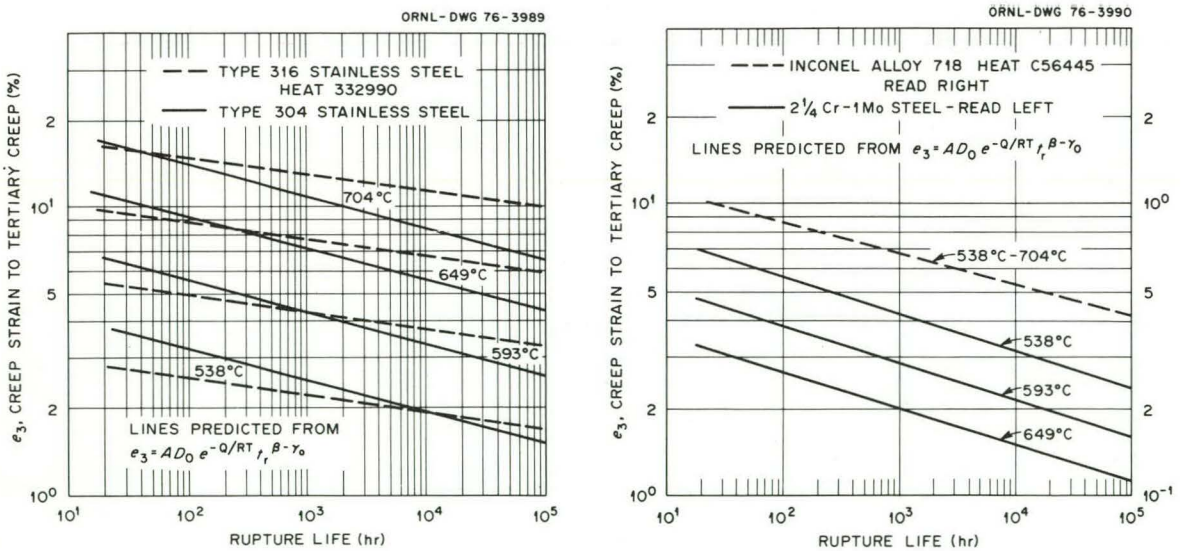

Fig. 27. Predicted Trends in Creep Strain to Tertiary Creep from Eq. (23).

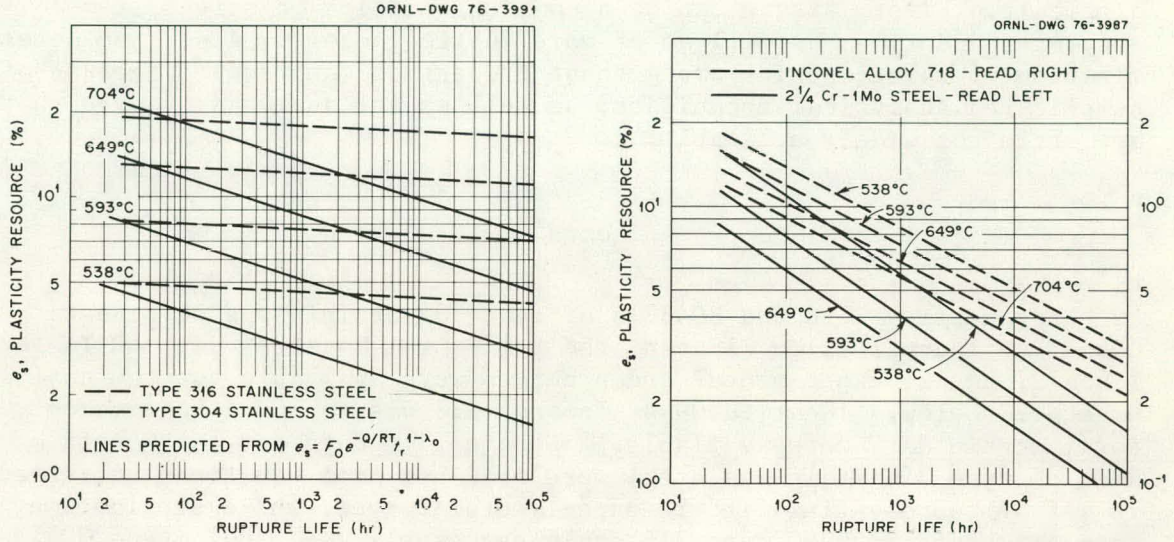

Fig. 28. Predicted Trends in Plasticity Resource from Eq. (12).

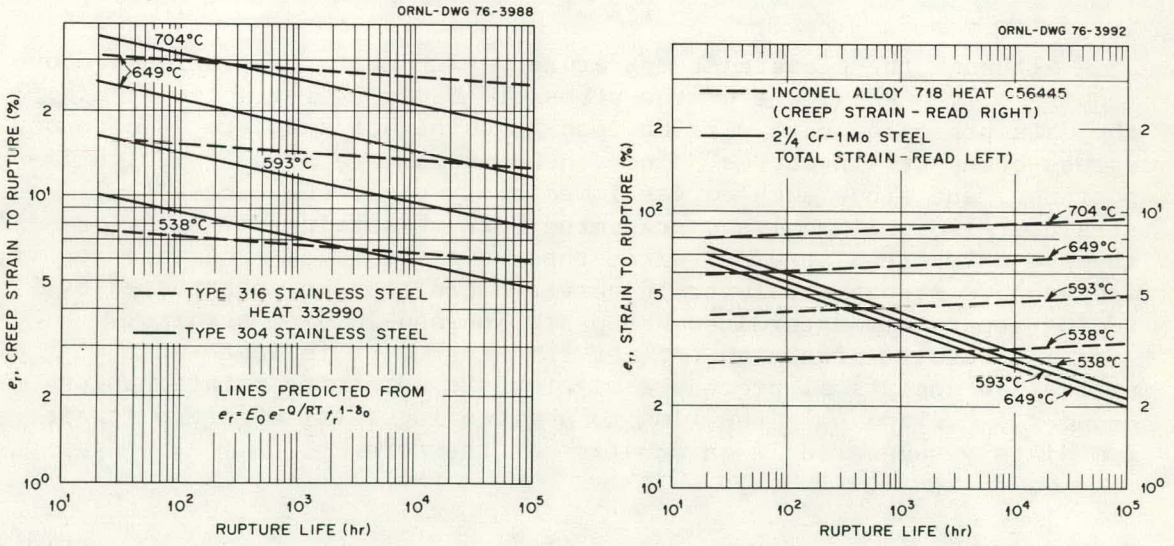

Fig. 29. Predicted Trends in Creep Strain to Rupture from Eq. (30).

STRAIN-TIME PREDICTIONS

Analysis of the third elevated-temperature design criterion — the stress to cause 1% inelastic strain in time t — is probably the most difficult. First, strain can be a complex function of stress, temperature, and time, as well as of more subtle factors. Also, the determination of relationships among these properties can require the use of complicated analytical techniques, as well as the analysis of data that are often not widely available.

Data

For heats 9T2796 and 8043813 of type 304 stainless steel, heat C56445 of Inconel alloy 718, and the 2 1/4 Cr-1 Mo steel data of Tables 1 and 2, actual experimental creep curves were available for the analyses presented below. (Heat Y8509 of Inconel 718 was not used because only total strain data were available.) Strain-time data for the Garofalo heat of type 316 stainless steel were obtained from equations presented in Ref. 7 representing fits to experimental curves, while strain-time data for heats 332990 (type 316 stainless steel) and 55697 (type 304) were obtained from such equations presented in Ref. 4.

Methods of Analysis

Although the elevated-temperature design criteria mentioned above require only a knowledge of the stress to cause 1% inelastic strain, the data presented here will be used to construct complete isochronous stress-creep-strain curves, since these curves are also of design importance, and since such curves immediately yield the stress to 1% strain. Also, all analyses presented here of strain-time behavior involve only creep strains, since these are the concern of this report. Isochronous stress-total-strain curves could then be constructed by adding separately determined creep strains and loading strains.

The results presented earlier in this report indicate that an attractive analytical procedure might be to determine relationships among t_r, $\dot{e}_m$, and t_x — the time to a given level (x) of creep strain. Immediately suggested is an equation of the form

$$t_x = G t_r^{\mu} , \tag{31}$$

where G and μ are constants, possibly dependent upon temperature. On the other hand, since t_x is a measure of flow rather than failure characteristics, the use of relationships between t_x and $\dot{e}_m$ is indicated, for instance

$$t_x = H\dot{e}_m^{-\varepsilon} \quad . \tag{32}$$

Exploratory investigations involving Eqs. (31) and (32) have indicated that reasonably good results can be obtained, especially for strain levels greater than about 0.5%. Figures 30 and 31 illustrate some of these results. However, for small values of strain, t_r and t_x can vary widely in magnitude, thus raising the possibility that the material condition at rupture might be considerably different from the condition after the accumulation of x% strain. Murphy[33] has found that Eq. (31) yields unsatisfactory results for 12 Cr-Mo-V steel, especially for small strain levels, although results at larger strains (>0.5%) were somewhat better. However, similar objections to Eq. (32) would not be as strong.

The method that appears to yield optimum results and the most information about material behavior is that described below. The method is based upon first determining an appropriate analytical function describing strain as a function of time. A very useful such function is the single rational polynomial equation:

$$e = \frac{Cpt}{1 + pt} + \dot{e}_m t \quad , \tag{33}$$

where e is the creep strain, t the time, C the transient creep strain, $\dot{e}_m$ the minimum creep rate, and p a parameter related to the sharpness of curvature of the primary region (see Fig. 32). The properties of this equation are fully discussed elsewhere,[34] including evidence that the equation does accurately describe the creep strain-time behavior of the materials discussed here.

The next step is to evaluate the stress and temperature dependence of Eq. (33). One approach might be to fit Eq. (33) to experimental curves, then to evaluate the resulting best fit values of C, p, and $\dot{e}_m$ as functions of stress and temperature. This approach has obtained some success by use of an equation equivalent to Eq. (33) for 2 1/4 Cr-1 Mo steel[10] and by use of a double exponential creep equation[4] for types 304 and 316 stainless steel. However, such analysis is quite difficult, and the results[4,10] are for limited data bases.

A better approach would be as follows. First determine $\dot{e}_m$ as a function of stress and temperature using all available relevant data (not merely best fit constants from available curves). Alternatively, $\dot{e}_m$ can be expressed as a function of t_r as described earlier in this report. At any rate, methods for prediction of $\dot{e}_m$ are fairly well established.

Then, for the prediction of C (see Fig. 32) one need merely know e_3, t_3, and $\dot{e}_m$, since by definition

$$C = e_3 - \dot{e}_m t_3 \quad . \tag{34}$$

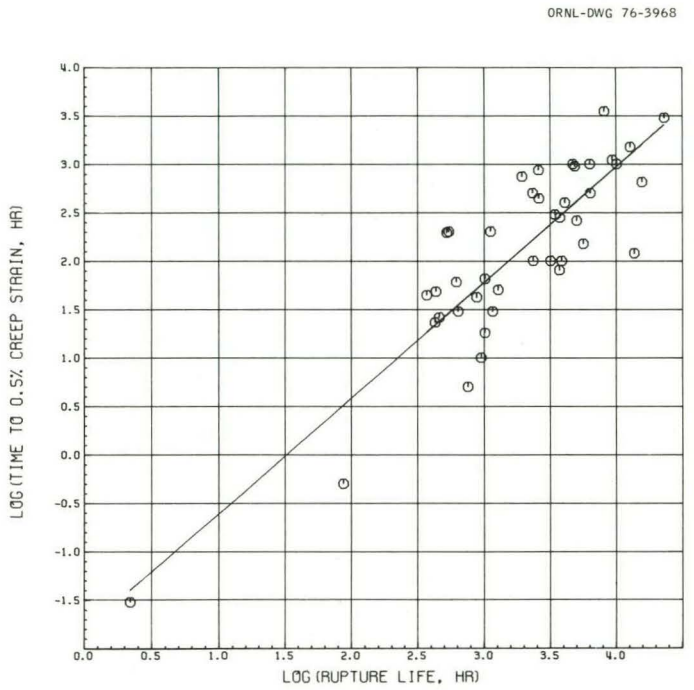

Fig. 30. Relationship Between Rupture Life and Time to the Accumulation of 0.5% Creep Strain for 2 1/4 Cr-1 Mo Steel at 593°C.

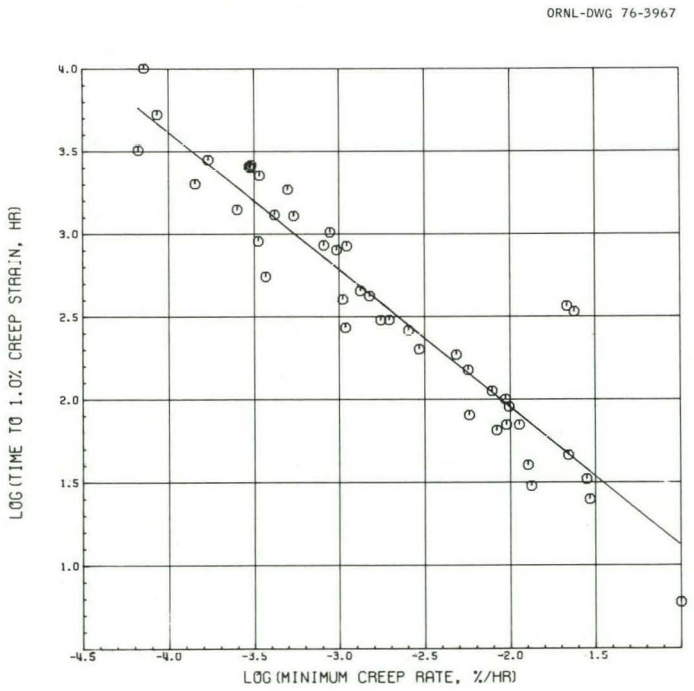

Fig. 31. Relationship Between Minimum Creep Rate and Time to the Accumulation of 1.0% Creep Strain for 2 1/4 Cr-1 Mo Steel at 593°C.

ORNL-DWG 76-3986

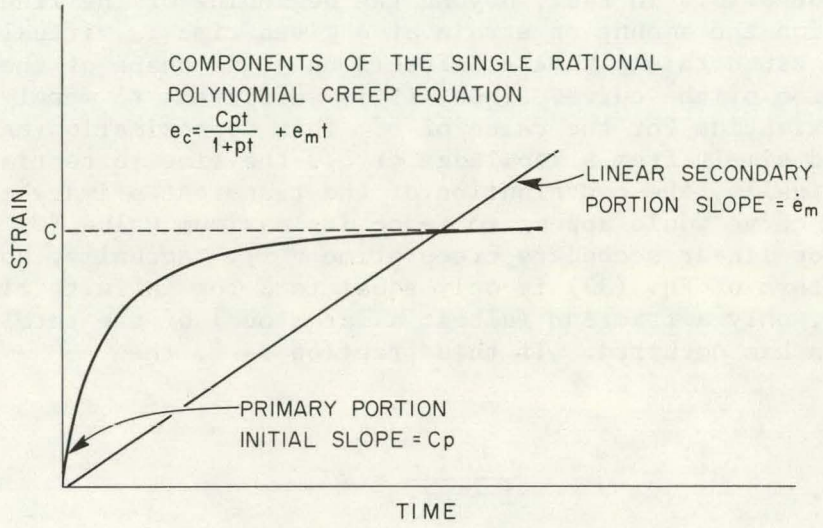

ORNL-DWG 76-3985

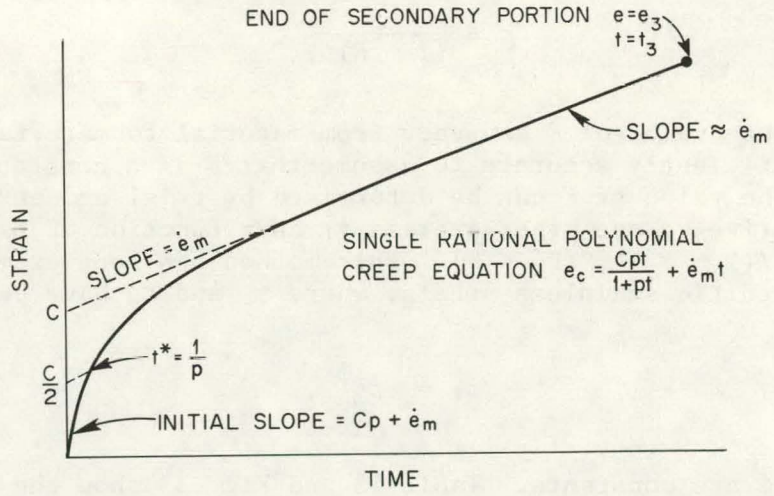

Fig. 32. Schematic Illustration of the Properties of the Single Rational Polynomial Creep Equation.

(For offset values of e_3 and t_3, $C = e_3 - \dot{e}_m t_3 - 0.2$). Therefore, since the previous sections of this report describe methods for prediction of e_3, t_3, and $\dot{e}_m$, these same methods allow prediction of C as a function of t_r or of t_r and $\dot{e}_m$, and thus of stress and temperature.

The only remaining step in expressing creep strain as a function of time, stress, and temperature is the determination of the parameter p. Fortunately, the total accumulated creep strain is relative insensitive to the value of p. In fact, beyond the beginning of the linear secondary creep portion the amount of strain at a given time is virtually independent of p, since this parameter affects only the shape of the primary creep portion of the curve. Thus, it is sufficient to merely obtain a good approximation for the value of p. This approximation can, in fact, be obtained simply from a knowledge of t_3, the time to tertiary creep.

Graphically, the contribution of the transient primary creep portion of a creep curve would appear to reach its maximum value (C) at the beginning of linear secondary creep, time = t_1. Actually, however, the transient term of Eq. (33) is only equal to C for infinite time, so that even at t_3, only a fraction (albeit a large one) of the total transient deformation has occurred. If this fraction is F, then

$$\frac{Cpt_3}{1 + pt_3} = FC \tag{35}$$

from which

$$p = \frac{F}{(1 - F)t_3} . \tag{36}$$

The appropriate value of F can vary from material to material, but it is possibly sufficiently accurate to assume that F is a constant for a given material. The value of F can be determined by trial and error.

Alternatively, one might express t_1 as a function of t_r and determine p as $F'/(1 - F')t_1$ ($F' < F$). This method has been examined only for the austenitic stainless steels, where t_1 and t_r have been related by

$$t_1 = Wt_r^{\phi} , \tag{37}$$

where W and ϕ are constants. Table 13 and Fig. 33 show the results of such a correlation for the austenitic stainless steels. The fit is reasonably good, but difficulties in determining t_1 from experimental curves and other factors make it possible to predict t_3 more accurately than t_1.

Finally, one might take the point t^* in Fig. 32, where the transient strain contribution is one-half its maximum. Thus, from Eq. (36)

Table 13. Results of Correlation Between Rupture Life and Time to the Onset of Secondary Creep[a]

Stainless Steel	Number of Data	Temperature Range of Data (°C)	W	ϕ	RMS[b]	R^2[c]
Type 304	170	538–704	0.095	1.043	0.414	89.1
Type 316	149	538–816	0.055	1.024	0.240	90.8

[a]Rupture life, t_r, and time to the onset of secondary creep, t_1, have been related by $t_1 = W t_r^{\phi}$.

[b]RMS in terms of $\ln(t_1)$.

[c]Coefficient of determination.

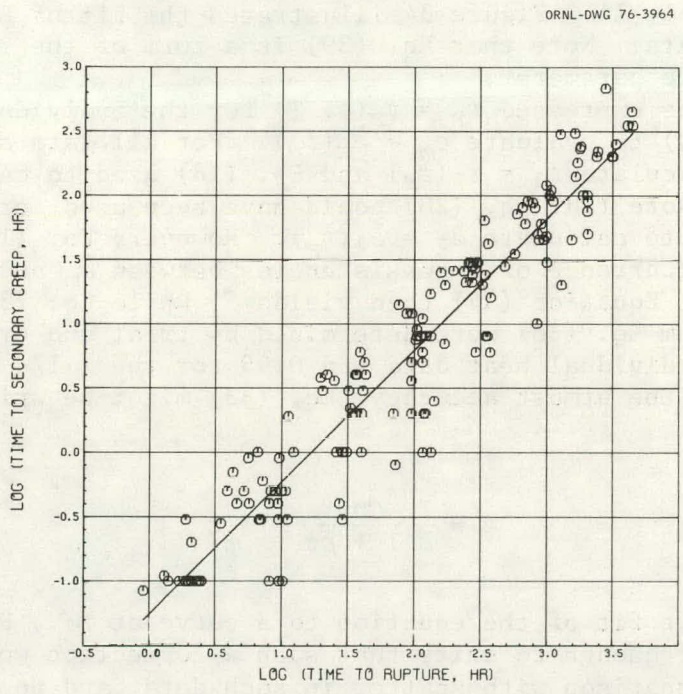

Fig. 33. Relationship Between Rupture Life and Time to the Onset of Secondary Creep for Type 316 Stainless Steel.

$$p = 1/t^* \ . \tag{38}$$

The value of t^* could probably be predicted from t_r by an equation similar to Eq. (37), but such a correlation has not been attempted for the current data sets.

Results

The specific procedures used for estimating the creep strain-time behavior of the current data sets are described below. For the 2 1/4 Cr-1 Mo steel, the equations for $t_r = t_r(\sigma, T)$ and for $\dot{e}_m = \dot{e}_m(\sigma, T, \tau)$ from Booker et al.[10] were used, where σ is stress, T is temperature, and τ is room-temperature ultimate tensile strength. For the remaining individual heat data sets, t_r was expressed as a function of σ and T by

$$\log t_r = \alpha_0 + \alpha_1\sigma + \alpha_2 \log \sigma + \alpha_3/T \ , \tag{39}$$

where α_0, α_1, α_2, and α_3 are constants estimated by least squares fits as shown in Table 14. Figure 34 illustrates the fit of Eq. (39) to experimental data. Note that Eq. (39) is a form of the Orr-Sherby-Dorn[22] time-temperature parameter.

Having thus expressed $t_r = t_r(\sigma, T)$ for the individual data sets, we used Eq. (10) to evaluate $\dot{e}_m = \dot{e}_m(t_r)$. For all data sets. Eq. (1) was used to calculate $t_3 = t_3(t_r)$ and Eq. (18) used to calculate $\dot{e}_3 = \dot{e}_3(\dot{e}_m)$. Note that Eq. (20) could have been used for the individual heat data sets to calculate $\dot{e}_3 = \dot{e}_3(t_r)$. However, Eq. (18) was used to minimize the occurrence of inconsistencies between $\dot{e}_m$ and $\dot{e}_3$ in extrapolated regions. Equation (34) then yields C, while Eq. (36) yields p. Values of F from Eq. (36) were determined by trial and error to be about 0.98 for the individual heat data and 0.95 for the 2 1/4 Cr-1 Mo steel.

To obtain the utmost accuracy, Eq. (33) might be written

$$e = \frac{1}{F}\frac{Cpt}{1 + pt} + \dot{e}_m t \tag{40}$$

to give an exact fit of the equation to a curve at t_3. However, the F values are near enough to unity that such a correction would be insignificant in comparison with scatter in such data, and no such corrections have been made.

Resulting predictions of strain-time behavior are shown in the form of isochronous stress-creep strain curves in Figs. 35 through 38. A fuller discussion of the results is reported elsewhere,[34] but several features are immediately apparent. First, from Figs. 35 and 36, note that the current method allows a prediction of heat-to-heat variations

Table 14. Results of Rupture Life Correlations[a]

Data Set	Number of Points	α_0	α_1	α_2	α_3	RMS
		Type 304 Stainless Steel				
Heat 55697	45	2.037	-6.222×10^{-5}	−3.987	1.722×10^{4}	0.021
Heat 9T2796 25 mm plate	58	3.626	-5.718×10^{-5}	−4.822	1.874×10^{4}	0.015
Heat 9T2796 51 mm plate	20	3.066	-5.393×10^{-5}	−4.966	1.962×10^{4}	0.014
Heat 8043813	24	−5.312	-1.067×10^{-4}	−4.233	2.667×10^{4}	0.023
		Type 316 Stainless Steel				
Garofalo et al.	132	−3.488	-1.018×10^{-4}	−2.813	1.895×10^{4}	0.018
Heat 332990	39	6.123	-4.248×10^{-5}	−5.414	1.962×10^{4}	0.027
		Inconel Alloy 718				
Heat Y8509	24	−33.38	-7.429×10^{-5}	3.504	2.331×10^{4}	0.029
Heat C56445	28	−41.84	-8.627×10^{-5}	5.253	2.412×10^{4}	0.008

[a]Determined by least squares fits using a model of the form $\log t_r = \alpha_0 + \alpha_1\sigma + \alpha_2 \log \sigma + \alpha_3/T$, where σ = stress (psi) and T = temperature (K). If σ is in MPa, multiply α_1 by 145.0 and add $2.161\alpha_2$ to α_0.

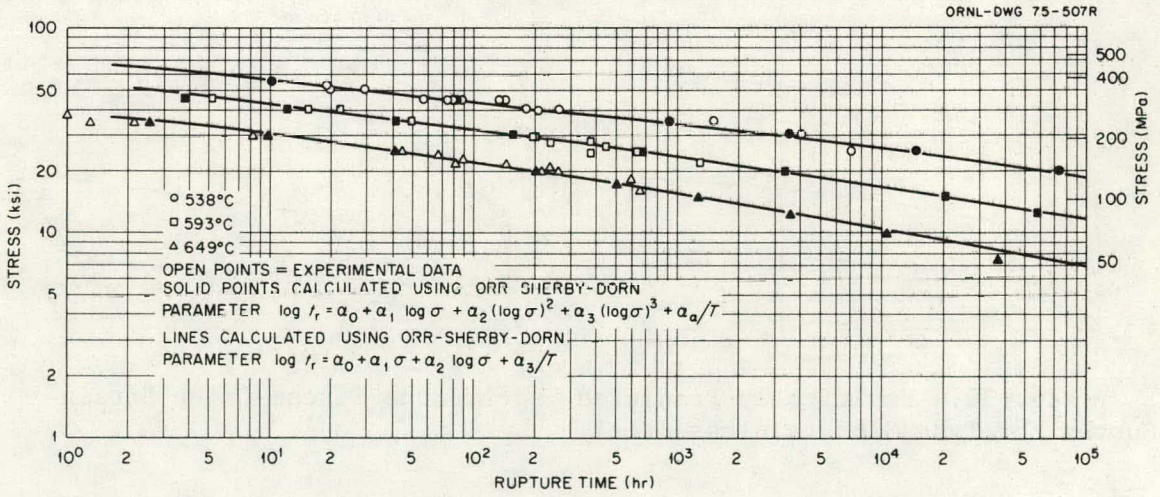

Fig. 34. Fit of Eq. (39) to Experimental Rupture Life Data for Type 304 Stainless Steel, Heat 55697.

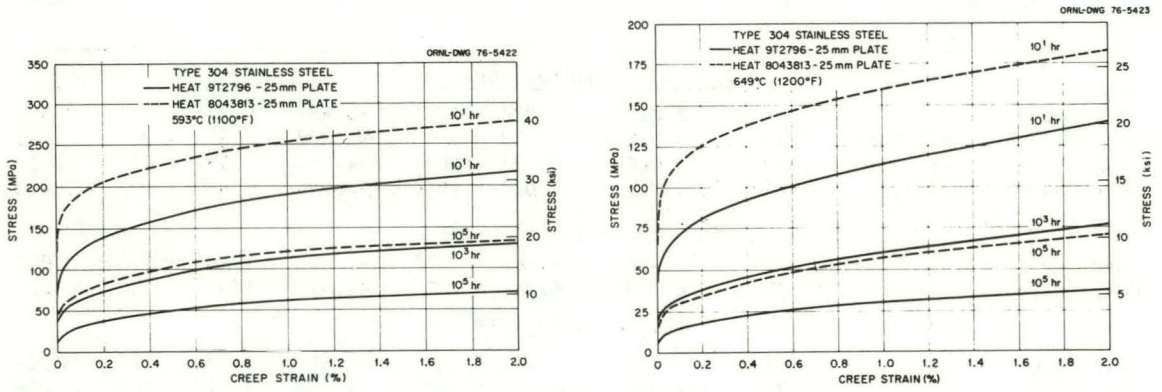

Fig. 35. Empirically Predicted Isochronous Stress-Creep Strain Curves for Type 304 Stainless Steel.

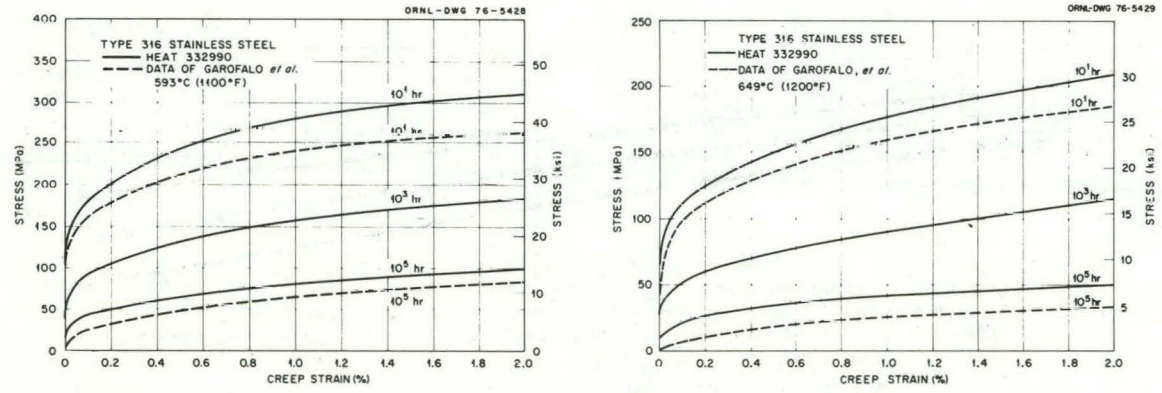

Fig. 36. Empirically Predicted Isochronous Stress-Creep Strain Curves for Type 316 Stainless Steel.

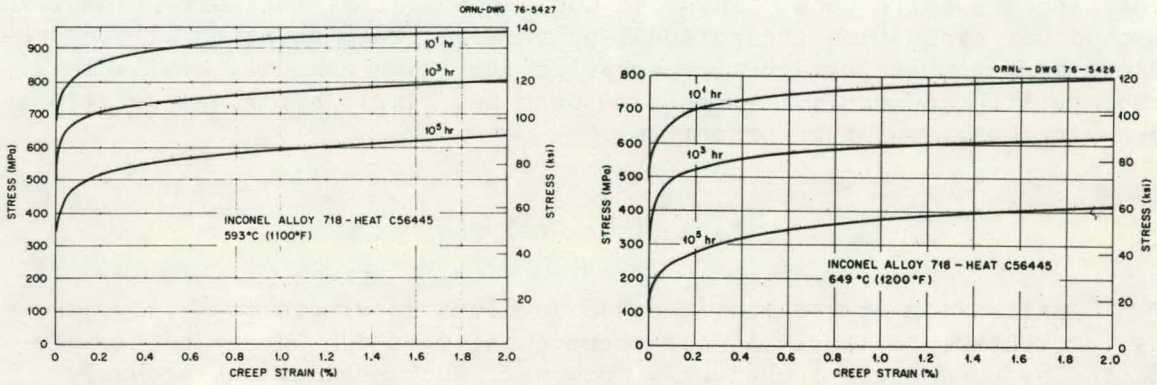

Fig. 37. Empirically Predicted Isochronous Stress-Creep Strain Curves for Inconel Alloy 718.

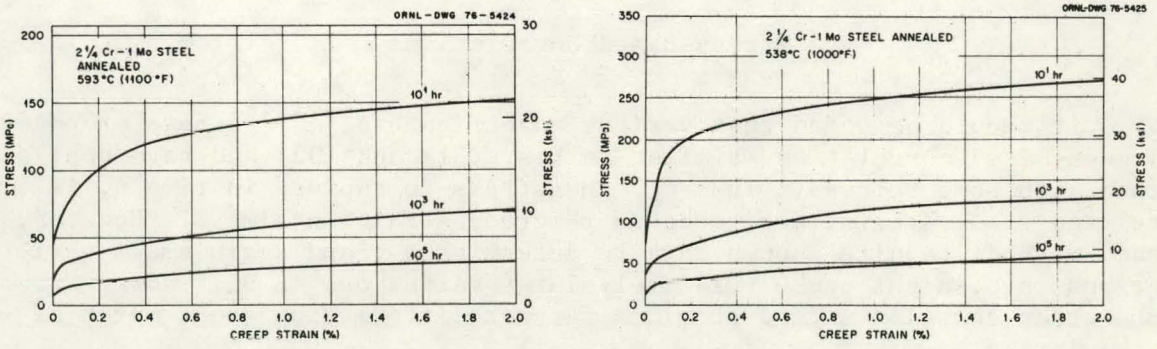

Fig. 38. Empirically Predicted Isochronous Stress-Creep Strain Curves for 2 1/4 Cr-1 Mo Steel.

in strain-time behavior, and, at least for the two austenitic stainless steels examined here, such variations can be large.[21] The most unusual feature is the apparently inconsistent shape of the curves for 2 1/4 Cr-1 Mo steel. This shape, however, is related to the tendency of this material to display nonclassical concave upward creep curves in many cases. Such a curve can still be described by Eq. (33) by making C negative, and such predictions appear promising. The complicated strain-time characteristics of this material are described in more detail.[34,35]

Figures 39 through 42 illustrate comparisons between predictions of strain-time behavior and actual data for the materials considered here. The fits are quite good. Thus, it would appear that the current empirical method for evaluating the rational polynomial creep equation allows prediction of complex strain-time behavior utilizing commonly available rupture life and minimum creep rate data and simple empirical relationships between these and other properties.

Parametric Analysis

Application of the above method involves knowledge of $\dot{e}_m$, e_3, and t_3. As shown previously,[18] all these quantities can be separately predicted by parametric techniques. However, such predictions probably require more data than the above empirical correlations, and are most effective only on an individual heat basis. Thus, the empirical methods presented above are expected to represent a more promising approach to predicting strain-time behavior.

Stress-Based Correlations

It should be noted that various investigators[30,33,36] have proposed stress-based correlations similar to Eqs. (31) and (32) and have applied them with some success. Thus σ_r, the stress to rupture in time t, is related to σ_x, the stress to cause x% creep strain in time t. However, such methods require enough data to determine σ_x, and again small variations in σ_x might cause relatively large variations in t_x. Moreover, the creep equation method provides far more information about material behavior.

Design Application

Clearly, the above analysis yields a useful method for determining the stress to cause 1% strain, and thus is an aid in determining elevated-temperature allowable stress levels. Minimum values can possibly be calculated simply by using average C and p values and substituting a statistically determined upper limit value of $\dot{e}_m$ in Eq. (33).

Beyond this, the ability to predict actual strain-time behavior is obviously of great utility in component design. Being able to make such

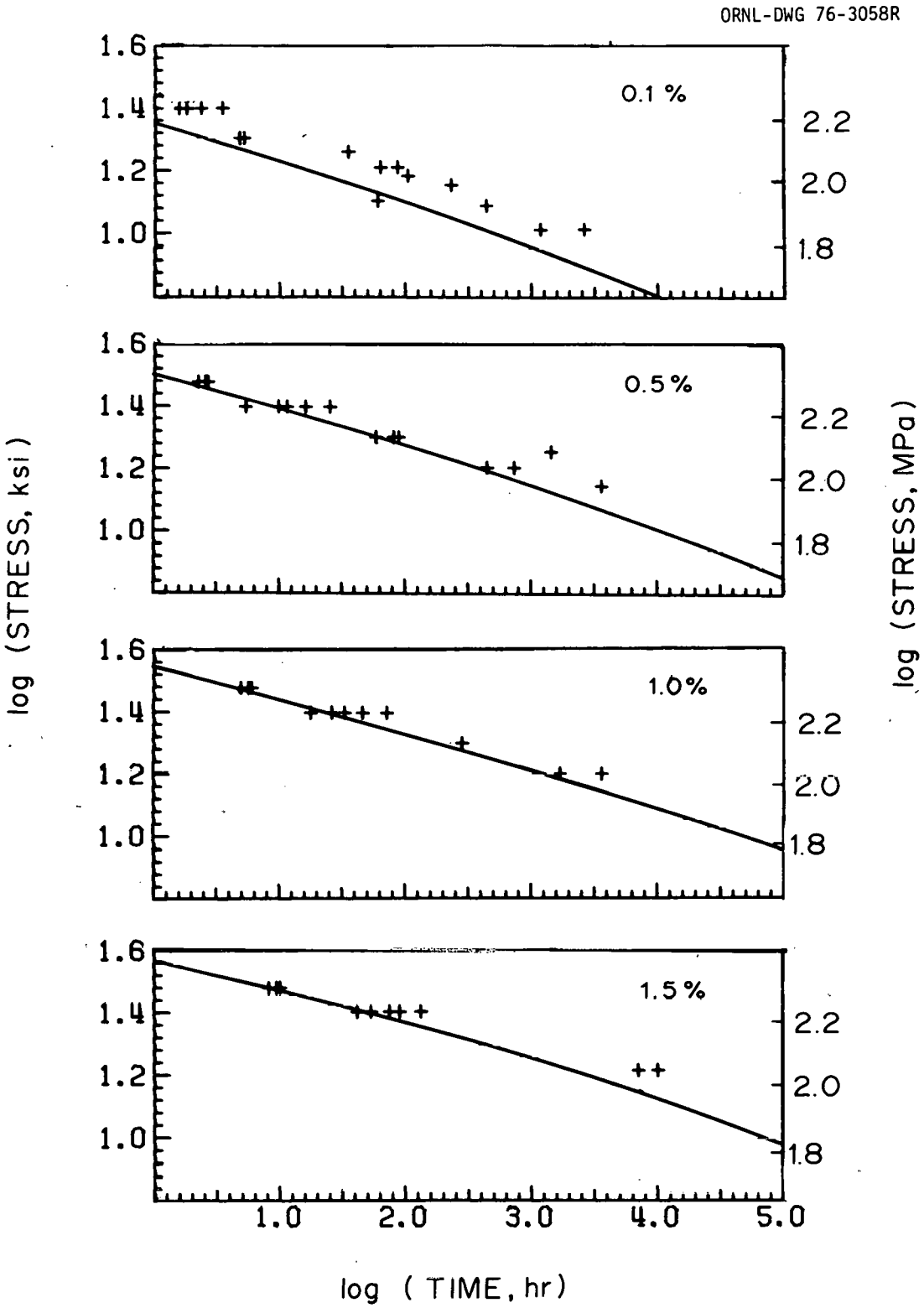

Fig. 39. Comparison of Empirical Predictions with Experimental Strain-Time Data for Heat 9T2796, 51-mm Plate, Type 304 Stainless Steel.

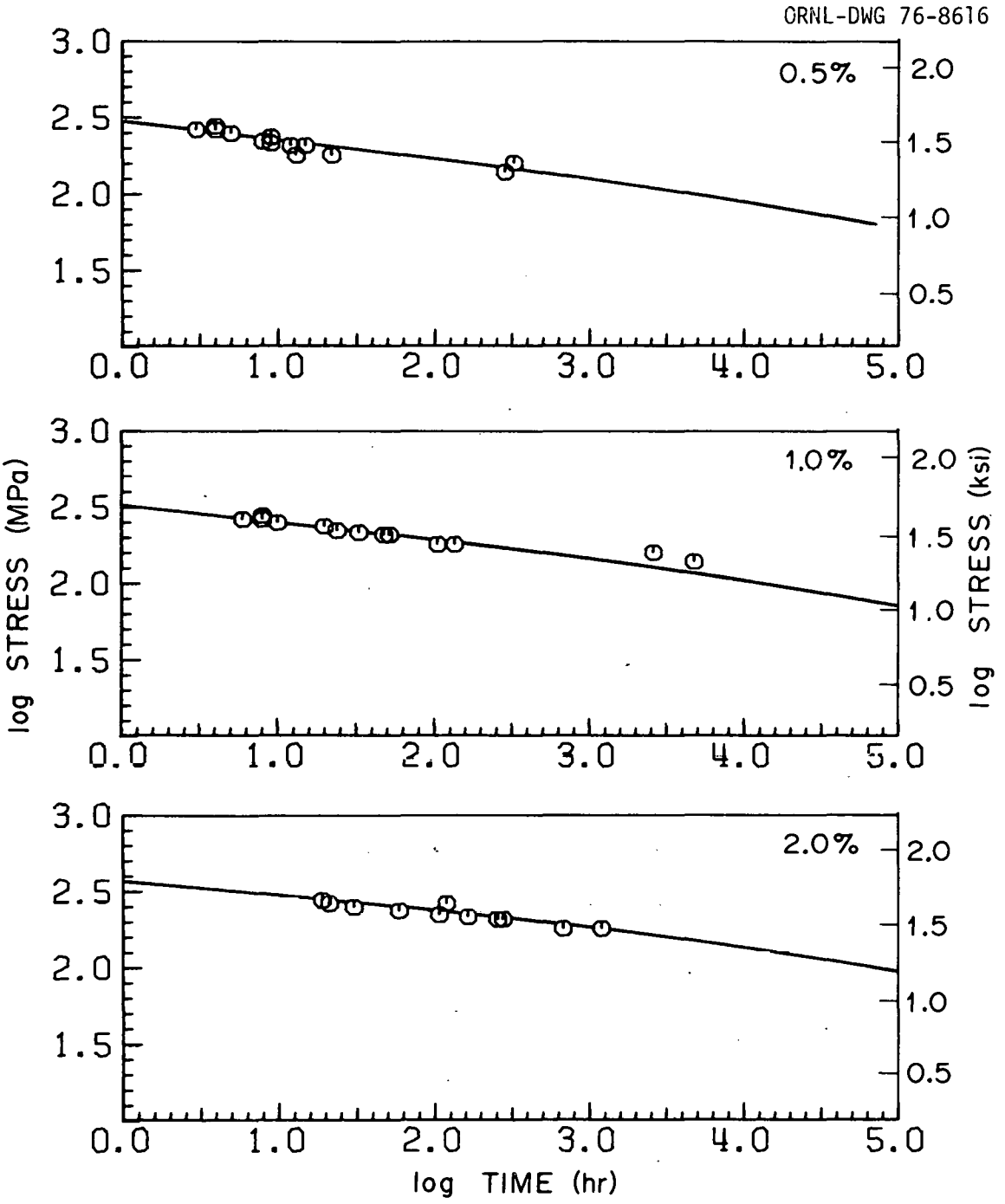

Fig. 40. Comparison of Empirical Predictions with Experimental Strain-Time Data for Heat 332990, Type 316 Stainless Steel.

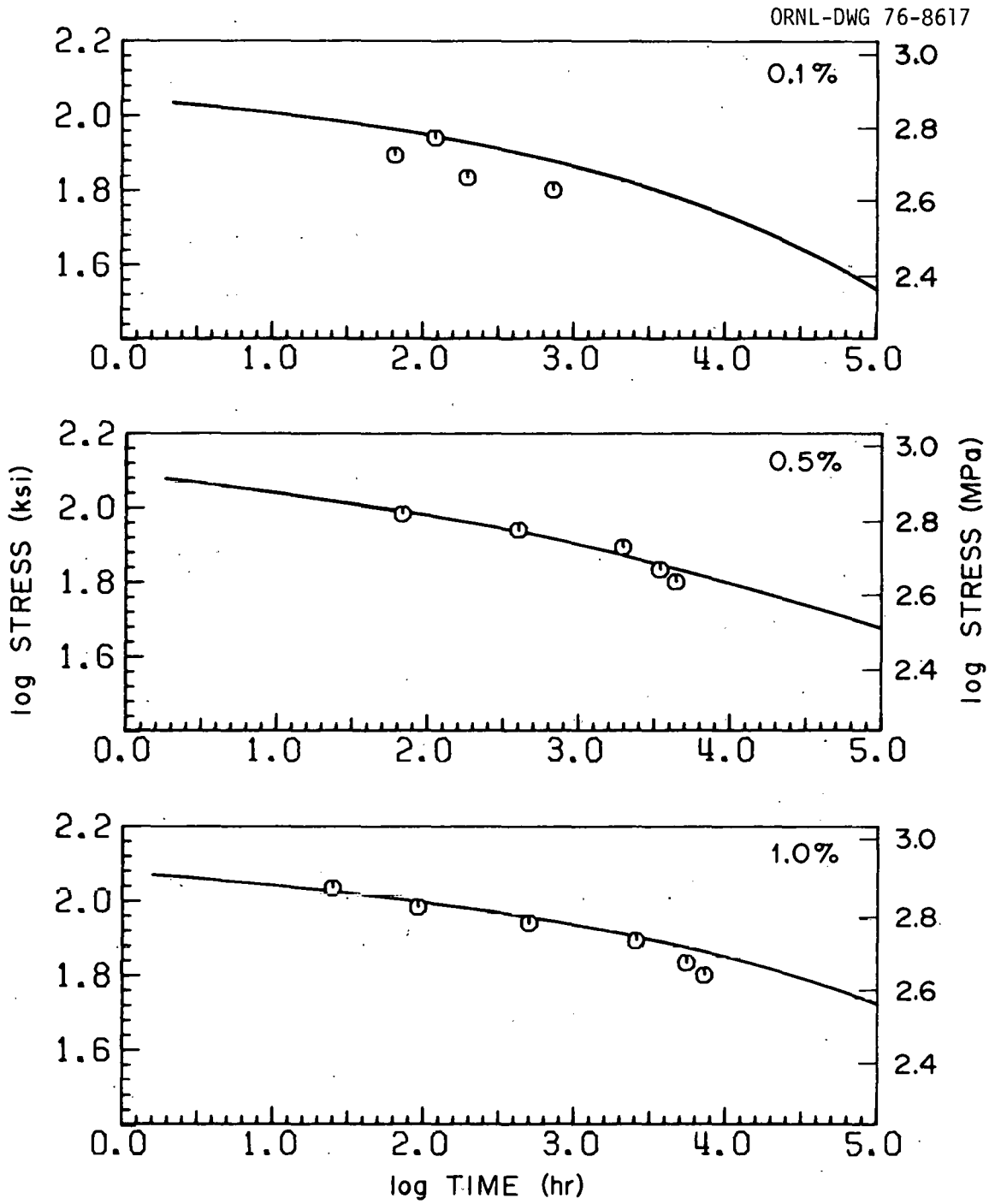

Fig. 41. Comparison of Empirical Predictions with Experimental Strain-Time Data for Heat C56445, Inconel Alloy 718.

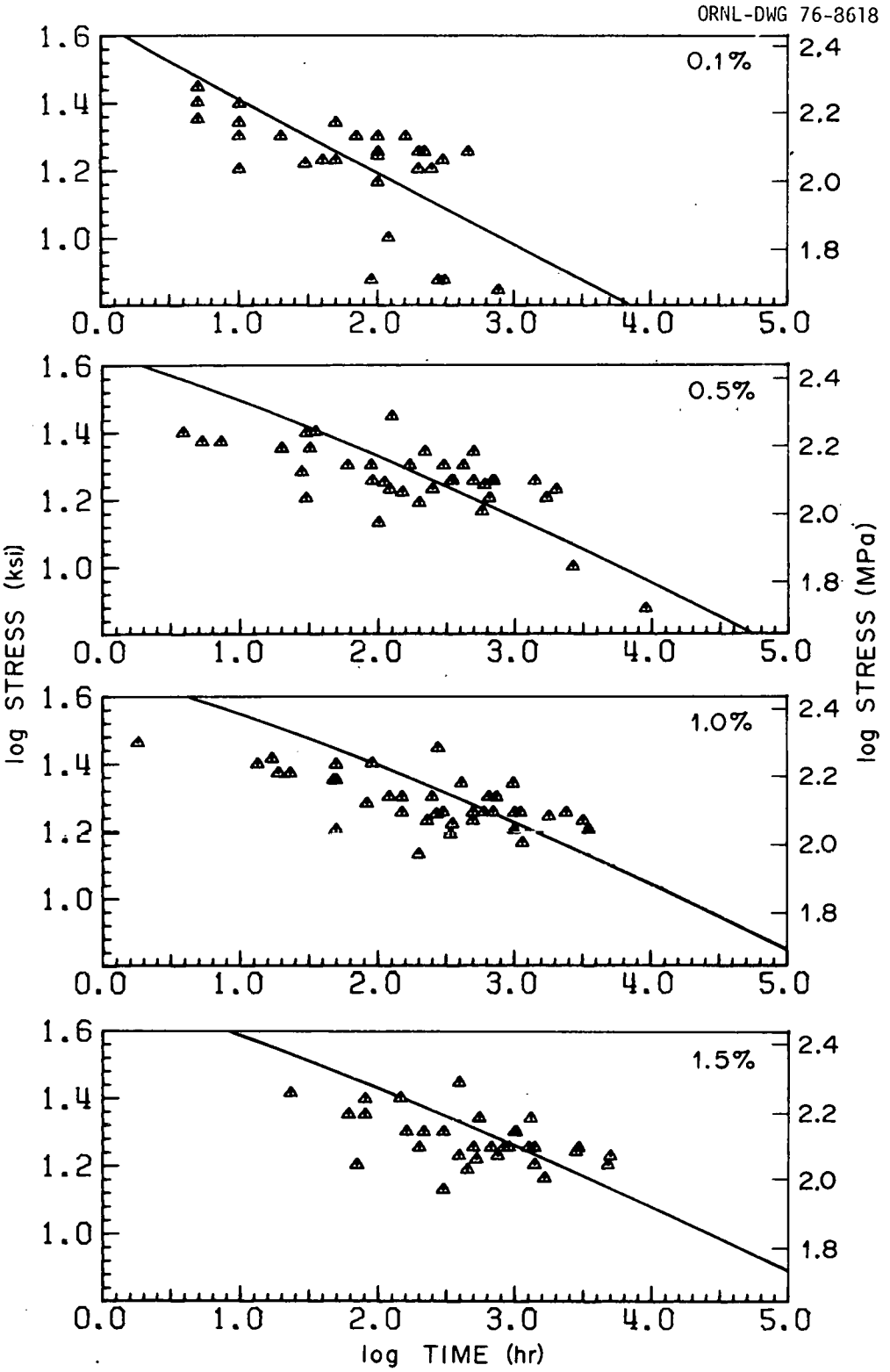

Fig. 42. Comparison of Empirical Predictions with Experimental Strain-Time Data for 2 1/4 Cr-1 Mo Steel.

predictions based on widely available data increases this utility. Finally, the uniquely simple yet flexible characteristics of the rational polynomial Eq. (33) add an extra bonus. The equation can predict classical creep curves or concave upward creep curves; it can be solved explicitly for time as a function of strain; and its individual parameters (C, p, $\dot{e}_m$) have clear physical interpretations.

SUMMARY

This report is a summary of some of the empirical relationships that can be used in relating different creep and creep-rupture properties of a material. It must be emphasized that these relationships are strictly empirical and that no fundamental physical significance has been attached to them. Therefore, extension of these relationships to other materials etc. must be done with caution. Still, for the materials and data considered here, the relationships appear to represent useful techniques for design applications. In particular, the following results have been obtained.

1. The time to tertiary creep, t_3, may be predicted from the rupture life, t_r, by $t_3 = At_r^{\beta}$.
2. The minimum creep rate may be estimated from the rupture life, although the relationship between the two is temperature sensitive.
3. Creep ductility can be estimated from the rupture life and minimum creep rate. In particular, the plasticity resource, the strain to tertiary creep, and the strain to rupture have been so estimated.
4. Strain-time behavior can be described by a simple rational polynomial creep equation. The parameters in this equation can be predicted from the rupture life and minimum creep rate.

ACKNOWLEDGMENTS

The authors would like to express their appreciation to D. O. Hobson, J. E. Selle, and C. R. Brinkman for reviewing the contents of this report. Thanks also go to S. Peterson for editing and Stephanie B. Davison for preparing the final manuscript.

REFERENCES

1. *Interpretations of the ASME Boiler and Pressure Vessel Code, Case 1592,* American Society of Mechanical Engineers, New York, 1974.

2. R. W. Swindeman, "Creep-Rupture Correlations for Type 304 Stainless Steel (Heat 9T2796)," pp. 1–30 in *Structural Materials for Service at Elevated Temperatures in Nuclear Power Generation,* MPC-1, ed. by A. O. Schaefer, The American Society of Mechanical Engineers, New York, 1975.

3. V. K. Sikka, H. E. McCoy, M. K. Booker, and C. R. Brinkman, "Heat-to-Heat Variation in Creep Properties of Types 304 and 316 Stainless Steel," *J. Pressure Vessel Technol.* 97(4): 243 (1975).

4. L. D. Blackburn, "Isochronous Stress-Strain Curves for Austenitic Stainless Steels," pp. 15–48 in *The Generation of Isochronous Stress-Strain Curves*, ed. by A. O. Schaefer, American Society of Mechanical Engineers, New York, 1972.

5. R. W. Swindeman and C. E. Pugh, *Creep Studies on Type 304 Stainless Steel (Heat 8043813) Under Constant and Varying Loads*, ORNL-TM-4427 (June 1974).

6. F. Garofalo, R. W. Whitmore, and F. Von Gemmingen, "Creep and Creep-Rupture Relationships in an Austenitic Stainless Steel," *Trans. Metall. Soc. AIME* 221: 310–19 (1961).

7. F. Garofalo et al., "Strain-Time, Rate-Stress, and Rate-Temperature Relations During Large Deformations in Creep," pp. 1-31–1-39 in *Joint International Conference on Creep*, The Institution of Mechanical Engineers, London, 1963.

8. J. R. Barker, E. W. Ross, and J. F. Radavich, "Long Time Stability of Inconel 718," *J. Met.* 20(1): 31–41 (January 1970).

9. C. E. Korth, Aerojet Nuclear Company, private communication, January 1975.

10. M. K. Booker, T. L. Hebble, D. O. Hobson, and C. R. Brinkman, "Mechanical Property Correlations for 2 1/4 Cr-1 Mo Steel in Support of Nuclear Reactor Systems Design," paper F 8/9 in *Transactions of the 3rd International Conference on Structural Mechanics in Reactor Technology* (London, UK, 1–5 Sept. 1975), Vol 2, Part F, Commission of the European Communities, Luxembourg, 1975. See also ORNL/TM-5329, to be issued.

11. Unpublished data from one of the authors (V. K. Sikka).

12. M. K. Booker and V. K. Sikka, *Interrelationships Between Creep Life Criteria for Four Nuclear Structural Materials*, ORNL-TM-4997 (August 1975).

13. J. B. Conway, *Stress-Rupture Parameters; Origin, Calculation and Use*, Gordon and Breach, New York, 1969.

14. S. S. Manson, "Time-Temperature Parameters — A Re-Evaluation and Some New Approaches," pp. 1–114 in *Time-Temperature Parameters for Creep-Rupture Analysis*, ASM Publication D8-100, American Society for Metals, Metals Park, Ohio, 1968.

15. H. P. Van Leeuwen, *Predicting Material Behavior Under Load, Time, and Temperature Conditions,* Report 513, North Atlantic Treaty Organization Advisory Group for Aerospace Research and Development (June 1965).

16. T. L. Hebble, ORNL, unpublished research.

17. W. E. Leyda and J. P. Rowe, *A Study of the Time for Departure from Secondary Creep for Eighteen Steels,* ASM Technical Report P-6.1, American Society for Metals, Metals Park, Ohio, 1969.

18. M. K. Booker, C. R. Brinkman, and V. K. Sikka, "Correlation and Extrapolation of Creep Ductility Data for Four Elevated-Temperature Structural Materials," pp. 108–45 in *Structural Materials for Service at Elevated Temperature in Nuclear Power Generation* (Proc. Symp. Houston, Nov. 30–Dec. 4, 1976), American Society of Mechanical Engineers, New York, 1975.

19. R. L. Klueh, *The Relationship Between Rupture Life and Creep Properties of 2 1/4 Cr-1 Mo Steel,* ORNL-TM-4522 (May 1974).

20. *ASME Boiler and Pressure Vessel Code, Section III, Nuclear Power Plant Components,* American Society of Mechanical Engineers, New York, 1975.

21. V. K. Sikka, H. E. McCoy, M. K. Booker, and C. R. Brinkman, "Heat-to-Heat Variation in Creep Properties of Types 304 and 316 Stainless Steels," *J. Pressure Vessel Technol.* 97(4): 243–51 (November 1975).

22. R. L. Orr, O. D. Sherby, and J. E. Dorn, "Correlations of Rupture Data for Metals at Elevated Temperatures," *Trans. Am. Soc. Met.* 46: 113–28 (1954).

23. G. J. Hahn and S. S. Shapiro, *Statistical Models in Engineering,* Wiley, New York, 1967, pp. 261–82.

24. W. H. Beyer, ed., *Handbook of Tables for Probability and Statistics,* Chemical Rubber Co., Cleveland, 1966, p. 34.

25. F. C. Monkman and N. J. Grant, "An Empirical Relationship Between Rupture Life and Minimum Creep Rate in Creep-Rupture Tests," *Proc. Am. Soc. Test. Mater.* 56: 593–605 (1956).

26. V. S. Ivanova, "Creep Ductility Criterion for Metals," *Zavod. Lab.* 21(2): 212–16 (1955); Brutcher Translation 4210.

27. I. A. Oding and V. S. Ivanova, "Analysis and Application of Certain Creep Criteria," *Vestn. Mashinostr.* 35(5): 62–66 (1955); Brutcher Translation 4211.

28. P. W. Davies and B. Wilshire, "An Interpretation of the Relationship Between Creep and Fracture," pp. 34–43 in *Structural Processes in Creep,* Iron and Steel Institute, London, 1961.

29. F. Garofalo, *Fundamentals of Creep and Creep Rupture,* Macmillan, New York, 1965, p. 204.

30. R. F. Gill and R. M. Goldhoff, "Analysis of Long Time Creep Data for Determining Long Term Strength," *Met. Eng. Q.* 10: 30–39 (1970).

31. M. K. Booker, V. K. Sikka, and C. R. Brinkman, *Predicting the Strain to Tertiary Creep for Elevated-Temperature Structural Materials,* ORNL/TM-5403, report in preparation.

32. R. M. Goldhoff, "Some Observations on the Extrapolation of High-Temperature Ferritic Steel Data," *J. Basic Eng.* 82(4): 848–53 (December 1960).

33. M. C. Murphy, "Rating the Creep Behavior of Heat-Resistant Steels for Steam Power Plant," *Met. Eng. Q.* 13: 41–50 (1973).

34. D. O. Hobson and M. K. Booker, *Materials Applications and Mathematical Properties of the Rational Polynomial Creep Equation,* report in preparation.

35. M. K. Booker, *Creep Strain-Time Characteristics of Annealed and Isothermally Annealed 2 1/4 Cr-1 Mo Steel,* report in preparation.

36. R. M. Goldhoff and R. F. Gill, "A Method for Predicting Creep Data for Commercial Alloys on a Correlation Between Creep Strength and Rupture Strength," *J. Basic Eng.* 94: 1 (1972).

APPENDIX

Methods for Testing Independence of Various Data Sets

THIS PAGE

WAS INTENTIONALLY

LEFT BLANK

The methods presented below may be used to determine whether different data sets (i.e., data at different temperatures, for different heats, etc.) may be treated together for purposes of fitting regression models similar to those used throughout this report. For clarity, Eq. (1) will be treated as an example, although the general method is equally applicable to any of the similar equations used in this report.

Method A

For an equation of the form

$$t_3 = A t_r^{\beta} , \tag{A1}$$

one would actually determine the least squares estimates of A and β by fitting to the data a model of the form

$$y = b_0 + b_1 x , \tag{A2}$$

where

$y = \log t_3$,
$x = \log t_r$,
$b_1 = \beta$,
$b_0 = \log A$.

Assume that initially the data at different temperatures etc. have been treated separately. Such a procedure will yield a residual sum of squares given by

$$\text{SSR} = \sum_{i=1}^{n} (y_i - \hat{y}_i)^2 , \tag{A3}$$

where y_i = experimental values of log t_3, $\hat{y}_i$ = predicted values of log t_3 from the fit equations, and n is the number of data. If m is the number of separate data sets (temperatures), $2m$ is the total number of regression constants to be estimated.

If it is now assumed that all the separate data sets can be treated together, the number of regression constants is reduced to 2, and the fit results in a residual sum of squares given by

$$SSW = \sum_{i=1}^{n} (y_i - \hat{y}_i^*)^2 \ , \qquad (A4)$$

where $\hat{y}_i^*$ = the new predicted values of log t_3.

Since this second analysis involves fewer constants, SSW will necessarily be larger than SSR. The difference SSW − SSR is the sum of squares due to the hypothesis that only one line is needed. Letting this assumption be the null hypothesis, one then can test this hypothesis using the variable

$$F = \frac{(SSW - SSR)/(2m - 2)}{SSR(n - 2m)} \ . \qquad (A5)$$

This variable is a random variable having an F distribution with 2 and $n - 2m$ degrees of freedom,

$$F = F_{\alpha}(2m - 2, \ n - 2m) \ . \qquad (A6)$$

Having obtained this F value, one can then find the corresponding significance level α by consulting tables or by using standard computer programs.

The level of significance, α, is the probability that one makes an error in rejecting the null hypothesis (i.e., the probability that one makes an error by assuming it necessary to use isothermal data fits). Whether a given α value thus indicates use of isothermal or combined fits depends upon the particular situation.

Method B

The same method can be applied to the assumption that β in Eq. (A1) is temperature independent, while A is temperature dependent. First, fit all the combined data using Eq. (A2). The resulting value of β can then be used as the standard value. The individual (isothermal) data sets can then be described by a model of the form

$$\log t_3 = b_0 + \beta \log t_r \ , \qquad (A7)$$

where b_0 will be different for each data set. Then, SSR is given by

$$SSR = \frac{\sum_{i=1}^{n} (y_i - \hat{y}_i)^2}{n - (m + 1)} \qquad (A8)$$

since there are now $m + 1$ regression constants. Then, the F value of interest is given by

$$F = F(m - 1,\ n - 2m) \ . \tag{A9}$$

Method C

Having fit separate data sets by Eq. (A2), one can individually examine variations in constants b_0 and b_1. Based on the assumption that the model in Eq. (A2) is correct, there exist specific values b_0* and b_1* of the constants that are the true values. The regression constants b_0 and b_1 are merely estimates of these true values based upon the available data. Separately constructed confidence intervals for b_0* and b_1* can be constructed as follows:

$$b_1 - \frac{t_{\alpha/2}\, s}{\sqrt{S_{xx}}} < b_1^* < b_1 + \frac{t_{\alpha/2}\, s}{\sqrt{S_{xx}}} \tag{A10}$$

and

$$b_0 - \frac{t_{\alpha/2}\, s \sqrt{\sum_{i=1}^{n} x_i^2}}{\sqrt{n S_{xx}}} < b_0^* < b_0 + \frac{t_{\alpha/2}\, s \sqrt{\sum_{i=1}^{n} x_i^2}}{\sqrt{n S_{xx}}} \ , \tag{A11}$$

where $t_{\alpha/2}$ is the value of the t distribution with $n - 2$ degrees of freedom at a significance level $\alpha/2$, s is the standard error of estimate of y, n is the number of data in the individual (isothermal) data set, x_i = the experimental values of log t_r, S_{xx} is defined below:

$$s = \sqrt{\frac{\sum_{i=1}^{n} (y_i - \hat{y}_i)^2}{n - 2}} \ , \tag{A12}$$

$$S_{xx} = \sum_{i=1}^{n} x_i^2 - \left(\sum_{i=1}^{n} x_i \right)^2 / n \ . \tag{A13}$$

These intervals may be interpreted to mean that the confidence is $(1 - \alpha)100\%$ that the true values of b_0* or b_1* lie within the interval.

If the confidence intervals about one of the constants b_0 and b_1 for two different data sets do not overlap, then the value of that constant for the two data sets is significantly different at the $(1-\alpha)100\%$ confidence level. If the invervals do overlap, the values may or may not be significantly different. However, some insight can be gained.

It should be noted that, in actuality, the values of b_0 and b_1 are not independent, and therefore this method is not rigorously valid, although it does provide a useful check. The method described below allows one to consider simultaneous variations in b_0 and b_1.

Method D

A more rigorous method than method C is that illustrated in Figs. A1 and A2). For a given data set Eq. (A2) is fitted to the data. Figure A2 shows the predicted line obtained from this fit along with upper and lower confidence limits. At a given confidence level (say 95%) the confidence that the true mean value of y at a given x lies within these confidence limits is that value (e.g. 95%). At a given value of x, x_0, the confidence interval about $\hat{y}$ is given by

$$\hat{y} \pm t_{\alpha/2} s \sqrt{\frac{1}{n} + \frac{(x_0 - \bar{x})^2}{S_{xx}}} \quad , \tag{A14}$$

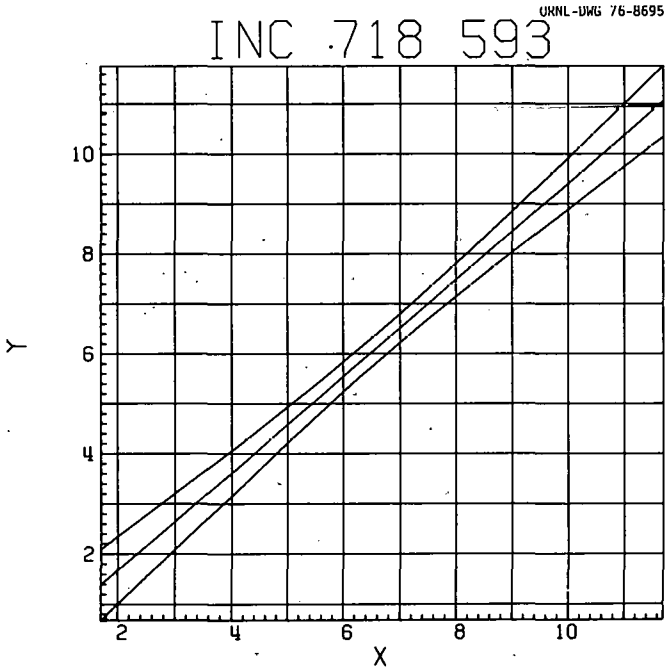

Fig. A1. Typical Best Fit Line from Eq. A2 with 95% Confidence Limits Shown.

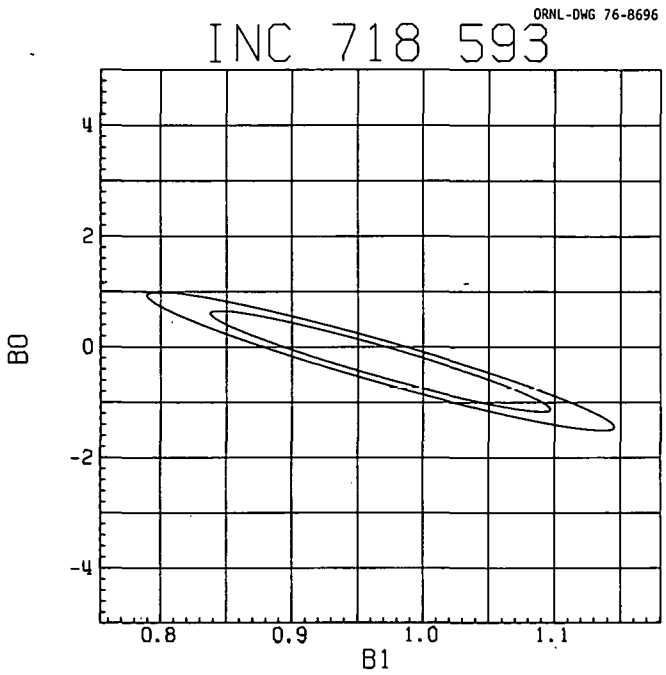

Fig. A2. Typical Confidence Ellipses Showing Possible Simultaneous Variations of Constants b_0 and b_1 from Eq. (A2). Inner curve: 95% confidence level. Outer curve: 90%.

where $\bar{x}$ is the arithmetic mean of the x values used $= \left(\sum_{i=1}^{n} x_i\right)/n$. The confidence is $(1 - \alpha)100\%$ that the true mean value of y lies within this interval.

Whatever the true values b_0* and b_1*, the true mean line (within the confidence level chosen) must lie within the confidence limits of Fig. A1, which, of course, restricts the values of b_0 and b_1. Figure A2 illustrates this restriction, where it is seen that a pair of values (b_0, b_1) must lie within a "confidence ellipse," the size of which depends upon the confidence level chosen. A study of the overlapping of these confidence ellipses yields information about possible differences between the b_0 and b_1 values of different data sets, as discussed above in connection with method C.

THIS PAGE

WAS INTENTIONALLY

LEFT BLANK

ORNL/TM-5399
UC-79b, -k
(Liquid Metal Fast
Breeder Reactors)

INTERNAL DISTRIBUTION

1–2. Central Research Library
3. Document Reference Section
4–10. Laboratory Records Department
11. Laboratory Records, ORNL RC
12. ORNL Patent Office
13. G. M. Adamson, Jr.
14. S. E. Beall
15. R. G. Berggren
16–25. M. K. Booker
26. C. R. Brinkman
27. E. E. Bloom
28. D. A. Canonico
29. J. A. Conlin
30. J. M. Corum
31. W. R. Corwin
32. F. L. Culler
33. J. E. Cunningham
34. J. H. DeVan
35. D. P. Edmonds
36. W. R. Gall
37. G. M. Goodwin
38. R. J. Gray
39. W. L. Greenstreet
40. W. O. Harms
41. T. L. Hebble
42–44. M. R. Hill
45. J. P. Hammond
46. D. O. Hobson
47. F. J. Homan
48. H. Inouye
49. P. R. Kasten
50. J. F. King
51. R. T. King
52. R. L. Klueh
53. J. M. Leitnaker
54. A. L. Lotts
55. C. T. Liu
56. R. E. MacPherson
57. W. R. Martin
58. H. E. McCoy, Jr.
59. H. C. McCurdy
60. C. J. McHargue
61. R. K. Nanstad
62. H. Postma
63. P. Patriarca
64. C. E. Pugh
65. P. L. Rittenhouse
66. T. K. Roche
67. J. L. Scott
68–72. V. K. Sikka
73. G. M. Slaughter
74. W. J. Stelzman
75. J. O. Stiegler
76. J. P. Strizak
77. R. W. Swindeman
78. D. B. Trauger
79. W. E. Unger
80. J. R. Weir, Jr.
81. G. D. Whitman
82. J. W. Woods
83. Paul M. Brister (consultant)
84. J. Moteff (consultant)
85. Hayne Palmour III (consultant)
86. J. W. Prados (consultant)
87. N. E. Promisel (consultant)
88. D. F. Stein (consultant)

EXTERNAL DISTRIBUTION

89–90. ERDA DIVISION OF REACTOR RESEARCH AND DEVELOPMENT, Washington, DC 20545

Director

91–92. ERDA OAK RIDGE OPERATIONS OFFICE, P.O. Box E, Oak Ridge, TN 37830

Director, Reactor Division
Research and Technical Support Division

93–325. ERDA TECHNICAL INFORMATION CENTER, Office of Information Services, P.O. Box 62, Oak Ridge, TN 37830

For distribution as shown in TID-4500 Distribution Category, UC-79b (Fuels and Materials Engineering Development); UC-79k (Components)

☆ U.S. GOVERNMENT PRINTING OFFICE: 1976-748-189/382